

**JIMMA UNIVERSITY**  
**JIMMA INSTITUTE OF TECHNOLOGY**  
**FACULTY OF MECHANICAL ENGINEERING**  
**SUSTAINABLE ENERGY ENGINEERING STREAM**

**Adjusting and Performance assessment of an  
elliptical dish (scheffler reflector). In case of an  
installed scheffler coffee roaster at Jimma University.**

A Research Submitted to the School of Graduate Studies of  
Jimma University for Partial Fulfillment of the Requirement for  
the Degree of Masters of Science in Sustainable Energy  
Engineering

By

Serawit Demeke

Advisor: Prof. Dr. Ancha Venkata Ramayya

Co-Advisor: - Mr. Jemal Worku (MSc.)

March 9, 2021



**JIMMA UNIVERSITY**  
**JIMMA INSTITUTE OF TECHNOLOGY**  
**FACULTY OF MECHANICAL ENGINEERING**  
**SUSTAINABLE ENERGY ENGINEERING STREAM**

**Adjusting and Performance assessment of an  
elliptical dish (scheffler reflector).**

**In case of an installed scheffler coffee roaster at  
Jimma University**

A Research Submitted to the School of Graduate Studies of Jimma  
University for Partial Fulfillment of the Requirement for the Degree of  
Masters of Science in Sustainable Energy Engineering

By

Serawit Demeke

Advisor: Prof. Dr. Ancha Venkata Ramayya

Co-Advisor: - Mr. Jemal Worku (MSc.)

March 9, 2021

## Declaration

This research work is my original work and has not been presented for a degree in any other university

Serawit Demeke  
Name

\_\_\_\_\_

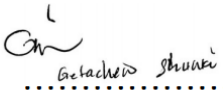
signature

\_\_\_\_\_

date

## Approval sheet

As a member of the Examination Board of the final Master of Science open defense, we certify that we have read and evaluated the thesis prepared by Serawit Demeke Asires entitled as “**Adjusting and Performance assessment of an elliptical dish (scheffler reflector). In case of an installed scheffler coffee roaster at Jimma University.**” We recommend that it could be accepted as a fulfilling the thesis requirement for the Degree of Master of Science in Mechanical Engineering (sustainable energy Engineering).

Prof. Dr. Ancha Venkata Ramayya	.....	.....
Advisor	signature	date
<u>Mr. Jemal Worku</u>	.....	.....
Co-advisor	signature	date
Dr. -Ing. Getachew Shunki	 .....	<u>November 14, 2021</u>
External Examiner	Signature	date
Sewayehu Tarekegn	.....	.....
Internal Examiner	Signature	date
Tarekegn Limore	.....	.....
Chairperson	signature	date

---

**Dedicated to my beloved  
family**

---

## Abstract

*Solar energy is now days one of the most important source of energy due to the scarcity (limited source of fossil fuel) and environmental crisis of carbon release from fossil fuel. It is clean and has no any negative impact on environment and ecology. As its source is a sun, it is renewable and free energy, which mostly used for power generation and heating purposes. Scheffler reflector is one of the various methods of harvesting the solar energy. These concentrators are lateral sections of paraboloids and provide fixed focus away from the path of incident beam radiations throughout the year. This study presents the performance assessment of scheffler reflector that installed at JUCAVM campus, which has a total surface area of 16m<sup>2</sup>.The scheffler reflector installed has attempted to roast coffee bean for commercial purposes, but due to the error that is committed during the installation, the reflector could not concentrate the ray coming from the sun. Hence, this study reveals the reason why the solar beam reflected dispersed instead of concentrating since scheffler reflector has a fixed focus throughout the year. Finally, after a successful assessment and corrective measures taken the dish has brought to concentrate the ray at the fixed focus and the required amount of heat for roasting coffee bean have been harnessed. Additionally, collecting solar data at the place of assessment and observing the effect of seasonal change on the reflector performance was also part of the assessment. After series of assessments, the scheffler reflector has concentrated the solar ray at the fixed focus. The other corrective measure has also been done on the absorber (roaster). Since the roaster could not distribute the required heat needed for roasting coffee then the improved absorber with better surface reaction for heat distribution capacity has raised. A temperature of 152<sup>0</sup>C has been achieved with the help of simulation using COMSOL MULTIPHYSICS software package to show how much heat distribution on the absorber has been achieved. Temperature distribution on the receiver of scheffler reflector has also been compared with the temperature on receiver of parabolic solar dish. During the sunny day, the maximum temperature of above 300<sup>0</sup>C and 210<sup>0</sup>C from absorber of scheffler reflector and parabolic solar dish have been observed during the assessment respectively.*

**Key words:** - Scheffler reflector (elliptical dish), parabolic dish, seasonal tracking, equinox, telescopic clamp, solar beam.

## **Acknowledgment**

I would like to thank first the almighty God for giving me this opportunity. Next, it is my pleasure to express the deepest appreciation his Excellency to Prof. Ancha Venkata Ramayya (PhD) for exposing me to such an indispensable work. Without his continuous support and guidance, as well as his encouragement during difficult periods the completion of this thesis work would not possible. Along with Prof. Venkata, I would like to thank Mr. Jemal Worku (MSc) my Co-Advisor for his careful review, comments and suggestions with regards to this thesis.

I am also very grateful to Mr. Tarekegn Limore (MSc) chairperson of sustainable energy engineering (SEE) who supported me to the completion of this thesis. I would also like to thank all the instructors who increased my knowledge in many areas, and who always gave me insightful responses to any questions and concerns. Last but not least, I would like to thank my friends who stand beside me to complete my work.

# Contents

Declaration .....	i
Approval sheet.....	ii
Abstract.....	iv
Acknowledgment.....	v
List of figures.....	viii
List of table .....	ix
Abbreviations & nomenclature .....	x
CHAPTER ONE .....	1
1. INTRODUCTION.....	1
1.1 Background .....	1
1.2 Basics of Solar Energy .....	2
1.3 Solar Energy Potential .....	3
1.4 Harnessing Solar Power.....	4
1.4.1 Photovoltaic systems .....	4
1.4.2 Concentrating Solar Power (CSP).....	4
1.5 Types of Concentrating Solar Power (CSP) .....	5
1.6 Statement of the problem .....	7
1.7 Objective .....	7
1.7.1 General objective .....	7
1.7.2 Specific objectives .....	7
1.8 Scope.....	8
1.9 Significance of the study .....	8
CHAPTER TWO .....	9
2. LITERATURE REVIEW .....	9
2.2 Scheffler Concentrator for Solar Cooking.....	12
CHAPTER THREE.....	15
3. METHODS AND MATERIALS.....	15
3.1 Study location .....	15
3.2 Methodology .....	16
3.3 Mathematical development of scheffler reflector.....	19
3.3.1 Procedure to Design the Concentrator Parabola .....	20
3.4 Distribution of crossbars on the reflector frame.....	23
3.4.1 Calculation of equations for crossbars ellipses.....	24
3.4.2 Calculation of depths and arc lengths for different crossbars .....	25



3.5 Fixed focus tracking .....	27
3.6 Moving with the Sun .....	29
3.7 Coffee roasting and its thermodynamic approach .....	30
3.7.1 Roasting process.....	31
3.9 Materials .....	39
3.9.1 Pyranometer .....	39
3.10 Data collected during the assessment .....	Error! Bookmark not defined.
3.12 Working principle .....	43
CHAPTER FOUR.....	44
<b>4. ANALYSIS AND EXPERIMENTAL EVALUATION OF ELLIPTICAL DISH (SCHEFFLER) COFFEE ROASTER.....</b>	<b>44</b>
4.1 Solar irradiation.....	44
4.2. Available Solar radiation: .....	44
4.3 Solar angles.....	47
4.3.1 The hour angle ( $\omega$ ) .....	47
4.3.2 Declination angle ( $\delta$ ):.....	48
4.4 Data gathered during the experiment .....	50
4.5 Why the ray from the elliptical dish was not focused .....	52
4.6 Remedies taken .....	53
Different measures have taken to harness the possible amount of energy from the reflector to roast coffee beans. These are: .....	53
4.7 Assessment procedure.....	53
4.8 Heat transfer analysis using Comsol Multiphysics .....	54
4.8.1 Heat transfer in comsol multiphysics .....	55
CHAPTER FIVE .....	57
<b>5. SIMULATION AND RESULT .....</b>	<b>57</b>
5.3 Interpretation of the result .....	62
CHAPTER SIX .....	63
<b>6. CONCLUSION AND RECOMMENDATION .....</b>	<b>63</b>
6.1 conclusion.....	63
6.2 Recommendation.....	64
References.....	65

## List of figures

Figure 1. 1 (i) Parabolic trough (ii) central receiver (iii) parabolic dish.....	6
Figure 1. 2 scheffler reflector (a) picture (b) schematic [1], [3] .....	6
Figure 2. 1 Schematic diagram of the Scheffler concentrator system .....	11
Figure 2. 2 a Scheffler technology tested in Ludhiana (Latitude.....	12
Figure 3. 1 Study location.....	15
Figure 3. 2 summary of methodology.....	16
Figure 3. 3 scheffler reflector .....	17
Figure 3. 4 Section of Scheffler reflector in a paraboloid [1].....	19
Figure 3. 5. Description of parabola of a Scheffler reflector. ....	21
Figure 3. 6 Description of the Scheffler reflector and crossbars on parabola curve...25	25
Figure 3. 7 Ellipse of the crossbar for the Scheffler concentrator .....	26
Figure 3. 8 Radius, depth and arc length details for the nth crossbar .....	27
Figure 3. 9 Hourly and seasonal tracking mechanism for Scheffler reflector [25].....	29
Figure 3. 10 Parabolas focusing the sunlight at a fixed focus by moving with the sun .....	30
Figure 3. 11 process of roasting coffee.....	32
Figure 3. 12 roasting coffee using scheffler reflector .....	36
Figure 4. 1: declination angle of sunrays .....	48
Figure 4. 2: hour angle Variation of the hour angle in a day [26] .....	48
Figure 4. 3 variation of declination of angle for all months of the year where n is gained from table 4. ....	49
Figure 4. 4 sunset hour angle variation in months .....	50
Figure 4. 5-Day length hours. ....	47
Figure 4. 6 monthly average Extraterrestrial radiation .....	46
Figure 4. 7 conduction heat transfer .....	55
Figure 5. 1 comparison data from both scheffler and parabolic dish.....	57
Figure 5. 2 comparison data from both scheffler and parabolic dish.....	58
Figure 5. 3 mesh of scheffler receiver .....	59
Figure 5. 4Figure 5.4 temperature distribution through receiver.....	60
Figure 5. 5 temperature distribution with time .....	61
Figure 5. 6 Roasting coffee using scheffler reflector.....	61

## List of table

Table 3. 1 Equations, semi-minor axis and semi-major axis of different crossbars....	26
Table 3. 2 Components and its Specification.....	38
Table 3. 3 specification of silicon pyranometer.....	39
Table 3. 4 data taken during the assessment on February 28/2020 ..	<b>Error! Bookmark not defined.</b>
Table 3. 5 data taken during the assessment on February 28/2020 ..	<b>Error! Bookmark not defined.</b>
Table 4. 1 Recommended Average Days for Months and Values of n by Months .....	44
Table 5. 1 Data collected on January 19/2020 .....	51
Table 5. 2 solar data collected on February 28/2020 .....	52

## Abbreviations & nomenclature

### **Abbreviations**

*DNI-direct normal incidence*

*STSC-scheffler type solar concentrator*

*SR-scheffler reflector*

*PVC-photovoltaic cell*

*Aa-aperture area*

*PTSC-parabolic trough solar collector*

*Tr Receiver temperature [°C]*

*Tsky Sky temperature [°C]*

*JUCAVM-Jimma University College of agriculture and veterinary medicine*

### **Nomenclature**

*$\epsilon$ - Emittance*

*$\delta$ - delta (declination angle) [°]*

*$\tau$  - transitivity*

*$\rho$ - Density, [kg/m<sup>3</sup>]*

*$\phi$ -Latitude [°]*

*$\omega_s$ - sunset hour angle [°]*

*$\alpha$ - solar altitude [°]*

*$\omega$ - Omega (hour angle) [°]*

*$\theta_z$ - zenith angle [°]*

*$\theta$ - Incident angle [°]*

*$\overline{H_0}$ - is the monthly mean daily radiation on a horizontal surface in the absence of the atmosphere*

*$\overline{N_s}$  – -is the monthly mean value of day length at a particular location,*

*$\overline{n_s}$ = - is the monthly mean daily number of hours of observed sunshine hours,*

*a, b is climatologically determined regression constant.*

*Aa-Area, [m<sup>2</sup>]*

*A<sub>r</sub>* -Receiver area

*C* -Concentration ratio

*d* -Diameter, [m]

*f* -focal

*I<sub>b</sub>* -Solar beam irradiation, [W/m<sup>2</sup>]

*I<sub>d</sub>* -Solar diffuse irradiation, [W/m<sup>2</sup>]

*I<sub>g</sub>* -Global solar irradiation, [W/m<sup>2</sup>]

*k* -Thermal conductivity, [W/mK]

*S* -sun

*Sh* - shadow

# CHAPTER ONE

## 1. INTRODUCTION

### 1.1 Background

In today's world, the energy requirements are met by burning of fossil fuel, which are, not only limited but also release pollutants that intoxicate the world and affect its climatic pattern. To reduce this dependence on the fossil fuel, scientists are making effort to use other sources of energy, which are present in abundance and are inexhaustible like sun, water etc. to generate electricity. These non-conventional sources of energy have the capacity to solve world energy crisis. Among the various non-conventional energy sources, solar energy contributes a large portion [5]. This history of using solar energy in daily life has been known since 1455 BC [6], still, complete utilization of this form of energy has not been possible.

The total amount of energy received by earth, from the sun, in an hour is more than the energy consumed in one year [24]. Solar energy striking the surface of Earth hits it directly or indirectly, through a number of reflections from the atmosphere. The key obstruction with solar energy is the erratic nature of its availability and the problem in capturing and storing it. Solar energy is also concentrated to limited parts of the world. Solar energy can be converted into electricity by either using photovoltaic cells or using concentrated solar power (CSP). Since its invention, photovoltaic cells have resolved a significant portion of the world's energy crisis and now contributes around 177 gigawatt or 1% of the world's electricity demands [8]. These cells are mixture of semi conducting materials which are used to convert solar energy directly into electricity using photoelectric and electrochemical processes [9]. With recent technological advancements maximum efficiency extracted from the photo-voltaic cells was increased to around 40% but the average efficiency remains around 15% [10]. Concentrated solar power, like photovoltaic cells, uses solar radiation to generate electricity. When CSP can also combined with thermal storage capacity, CSP plants can provide flexibility for grid energy because of the large capacity of thermal storage to generate electricity even when sun is blocked by the cloud or sundown [7, 8]. Depending on the use, there can be different ways to concentrate solar power to a point. For commercial purposes, where the temperature at the focus point needs to be high, use of parabolic through or central tower. Parabolic through and central towers are

widely used because of high temperature generation at the concentrated point. But, these are not practical as almost all parabolic concentrators have rigid structure and the focus. This motivated the Scheffler to come up with a design where hot focus is available at a fixed place so that solar energy can be contentedly used. He developed the Scheffler reflector in village workshops of India and Kenya so that this technology is in reach of everyone [11]. Scheffler [12] developed a special Scheffler reflector with  $50\text{m}^2$  surface area to heat a 2m long cremation chamber at  $700\text{ }^\circ\text{C}$ . Then different researchers started developing the Scheffler dish, which finds its application in the households for boiling water, cooking food and in medical applications [11–15].

## **1.2 Basics of Solar Energy**

The source of all solar energy is the sun and all life on the earth depends on it. Knowledge of the quantity and quality of solar energy available at a specific location is of prime importance for the design of any solar energy system. Although the solar radiation (insolation) is relatively constant outside the earth's atmosphere, local climate influences can cause wide variations in available insolation on the earth's surface from site to site. In addition, the relative motion of the sun with respect to the earth will allow surfaces with different orientations to intercept different amounts of solar energy [15]. The sun is a sphere of intensely hot gaseous matter with a diameter of  $1.39 \times 10^9\text{m}$  and is  $1.5 \times 10^{11}\text{m}$  from the earth, on the average [16]. The earth revolves around the sun every 365.25 days in an elliptical orbit, with a mean earth-sun distance of  $1.496 \times 10^{11}\text{m}$  ( $92.9 \times 10^6$  miles) defined as one astronomical unit (1 AU). This plane of orbit is called the ecliptic plane. The earth's orbit reaches a maximum distance from the sun, or aphelion, of  $1.52 \times 10^{11}\text{m}$  ( $94.4 \times 10^6$  miles) on about the 3rd of July [1].

The minimum earth-sun distance, the perihelion, occurs on about January 2nd, when the earth is  $1.47 \times 10^{11}\text{m}$  ( $91.3 \times 10^6$  miles) from the sun. Solar energy will provide an ever-increasing fraction of our future energy requirement. Even if solar radiation is abundant and renewable, it is diffuse. The temperature from this diffuse source is sufficient to provide domestic hot water or home heating, but much higher temperature is necessary to displace fossil fuels for production of electricity or other industrial applications. Thus solar radiation must be concentrated to produce this elevated temperature; it must also be collected and moved to the point of use. The use of solar energy to cook food presents a viable alternative to the use of fuel wood, kerosene, and other fuels [16].

### 1.3 Solar Energy Potential

Solar energy has the greatest potential of all the sources of renewable energy and if only a small amount of this form of energy is used, it will be one of the most important supplies of energy. Energy comes to the earth from the sun. Solar energy keeps the temperature of the earth above that in colder space, and causes current in the atmosphere and in the ocean, and the rain-cycle, and generates photosynthesis in plants [10] [21].

The solar power at the earth's atmosphere is  $10^{17}$  watts, whereas the solar power on earth's surface is  $10^{16}$  watts. The total worldwide power demand of all needs of human activities is  $10^{13}$  watts. Therefore, the sun can give 1000 times more power than what we need. If we can use 5% of this energy, it will be 50 times what the world will require. Attempts have been made to utilize energy in raising steam, which may be used in driving the prime movers for the purpose of generation of electrical energy. However on account of large space required, uncertainty of availability of energy at constant rate due to clouds, winds, mist etc. there is limited application of this source in the generation of power. Now a days the drawbacks as pointed out that the energy cannot be stored and it is a dilute form of energy etc. are out dated arguments, since the energy can be stored by producing hydrogen, or by storing in other mechanical or electrical thermal storage devices, or it can be stored in containers of chemicals called phase changing solutions. These solutions store large quantities of heat in a relatively small volume [10] [32].

The facts speak in favor of solar energy, that world's reserves of coal, oil and gas will be exhausted within a few decades. Nuclear energy involves considerable hazards and nuclear fusion has not yet overcome all the problems of even fundamental research, compared with these technologies, the feasibility of which is still uncertain and contested. The applications of solar energy, which are enjoying most success today, are [15]:

- a) Heating and cooling of residential building
- b) Solar water heating and solar distillation on a small community scale
- c) Solar drying of agricultural and animal products
- d) Salt production by evaporation of seawater or inland brines
- e) Solar cookers



- f) Solar engines for water pumping
- g) Food refrigeration
- h) Wind energy, which is indirect source of solar energy
- i) Solar furnaces
- j) Solar photovoltaic cells, which can be used for conversion of solar energy directly into electricity or for water pumping in rural areas
- k) Solar thermal electric power generation by:
  - Solar ponds
  - Steam generators heated by rotating reflectors (heliostats mirrors by tower concept
  - Reflector with lenses and pipe for fluid circulation (cylindrical parabolic reflectors) Etc.

## **1.4 Harnessing Solar Power**

The most abundant and convenient source of renewable energy is solar which can be harnessed in methods, either Photovoltaic (PV) or Concentrating Solar Power (CSP) technology.

### **1.4.1 Photovoltaic systems**

When certain semi-conducting materials, such as silicon, are exposed to sun light, they generate small amounts of electricity. This process is known as the photoelectric effect. The photoelectric effect defines the liberation or ejection of electrons from the surface of a metal in response to light. It is the basic physical process in which photovoltaic (PV) cell converts sunlight to electrical energy. Solar cells are just too expensive hence; photovoltaic cannot compete economically with other conventional power generators. Moreover, if the photovoltaic system is assumed to have a 100% efficiency, then the maximum power that can be generated shall never get more than 1 kW per m<sup>2</sup> of solar cells. Thus, it is not an effective method [10] [21].

### **1.4.2 Concentrating Solar Power (CSP)**

It is a promising technology for power generation in which the solar radiation is concentrated to generate high temperature for producing a solar thermal power plant.

With an average annual direct normal irradiance (DNI) of 2,000kWh/m<sup>2</sup> the area required to generate 100MW of power is about 2km<sup>2</sup>. Ethiopia receives an average annual DNI of nearly 5000 – 7000Wh/m<sup>2</sup> according to region and season and thus has great potential for the use of solar energy, which is sufficient to operate concentrating solar power plants (CSP) [16].

### **1.5 Types of Concentrating Solar Power (CSP)**

In concentrating solar power (CSP) technology, sun's direct normal irradiation is concentrated to produce heat with temperature ranging from 400°C to 1,000°C [8]. This heat is used to produce electricity by conventional steam cycle, or combined cycle, or Stirling engine or it is used in solar cooking. Based on the process of collecting and concentrating solar radiation, the CSP can be categorized into following major types [21] [31]

- i. Parabolic Trough:** Parabolic trough-shaped mirror reflectors are used to concentrate sunlight on to thermally efficient receiver tubes placed in the trough's focal line. A thermal transfer fluid, such as synthetic thermal oil, is circulated in these tubes. Heating the oil to 400°C by the concentrated sun's rays, this oil is then pumped through a series of heat exchangers to make superheated steam. The steam then is converted to electrical energy [10].
- ii. Central receiver or solar tower:** A circular array of heliostats (large individually tracking mirrors) is used to concentrate sunlight on to a central receiver mounted at the top of a tower. A heat-transfer medium in this central receiver absorbs the highly concentrated radiation reflected by the heliostats and changes it into thermal energy to be used for the subsequent generation of superheated steam for turbine operation [10].
- iii. Linear Fresnel reflector (LFR):** A Linear Fresnel Reflector (LFR) array is a line focus system similar to parabolic troughs in which solar radiation is concentrated on an elevated inverted linear absorber using an array of nearly flat reflectors. An LFR can be designed to have similar thermal performance to that of a parabolic trough per aperture area, although recent designs tend to use less expensive reflector materials and absorber components, which reduce optical performance and thus, thermal output [31].

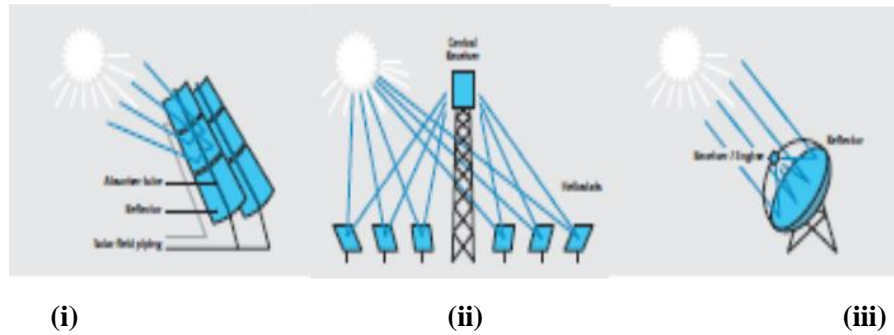


Figure 1. 1 (i) Parabolic trough (ii) central receiver (iii) parabolic dish

**iv. Parabolic Dish (Scheffler Solar Concentrators):** is a dish-shaped reflector, used to concentrate sunlight on to a receiver located at the focal point of the dish. The concentrated beam radiation is absorbed into the receiver to heat a fluid or gas (air) to approximately 1020°C [10]. The following section deals about Scheffler concentrators.

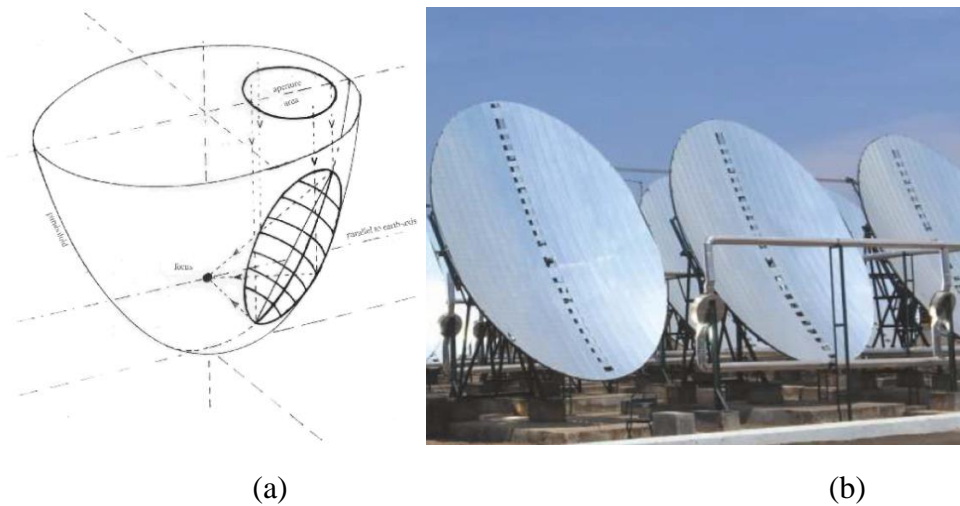


Figure 1. 2 (a) scheffler reflector section in parabola (b) manufactured scheffler reflector

Scheffler dish reflects light in two dimensions concentrating it to a single point. This paper attempted to assess Scheffler dish that installed at Jimma University agricultural campus. Invented by Wolfgang Scheffler, Scheffler reflector is a system of harvesting the solar energy. As depicted in Figure 1.2, Scheffler collector is a collector, which tracks the movement of the sun thus focusing sunlight on a focal point, which is fixed [16]. Scheffler reflectors are fixed focus, polar-axis parabolic solar concentrators that can achieve significant concentration factors at relatively low cost. The technology is widespread in India, and gaining popularity for medium scale solar cooking and process

steam generation. Among other features, the reflectors need a flexible structure to cope with the seasonal changes of the position of the sun.

Two telescopic bars fixed to the vertical ends of the reflector, which have to be adjusted manually every 3 to 5 days in order to get a good optical performance, accomplish deformation of the structure. Reports show that some operators do not perform this often enough, because of the trouble of having to climb to the structure and adjusting telescopic supports in an iterative manner. The goal of the assessment will be to adjust the upper side of mirror automatically upon adjustment of the lower telescopic bar.

### **1.6 Statement of the problem**

The coffee roaster that has already installed at Jimma University College of agriculture is not working due to unidentified factors. To fix the problem why the reflector cannot collect the solar irradiation coming from the sunlight to the given focal point has to be known. Therefore, daily measurement of the receiver performance is important to identify whether the problem is installation problem, position of sun (as sun changes its position when season changes) or design of the receiver (roaster) to harness maximum possible amount of energy from the roaster.

### **1.7 Objective**

The Performance assessment of elliptical dish (scheffler) coffee roaster has both general and specific objectives.

#### **1.7.1 General objective**

To adjust and Performance assessment of an elliptical dish (scheffler reflector) In case of an installed scheffler coffee roaster at Jimma University.”

#### **1.7.2 Specific objectives**

- To find the focal point of elliptical dish (scheffler) coffee roaster.
- To assess the effect of seasonal change of sun’s position on a receiver performance
- Adjusting the reflector using corrective tracking system
- Harness maximum amount of energy in the form of heat used for roasting coffee.

## **1.8 Scope**

Even if the assessment of elliptical dish reflector is broad, the process to be followed are limited certain activities.

- Adjusting the elliptical dish reflector to a point where the exact focal point is gained.
- Recording the daily solar incident and compare it with the time of the day.
- To figure out the possible solution of solar coffee roasting mechanism
- Comparing the performance of Scheffler reflectors with solar dish concentrator

## **1.9 Significance of the study**

The findings of this study will redound to the benefit of society considering that solar energy plays an important role as an alternative source of green energy. The greater demand for solar energy as a source of green energy justifies the need for more effective environmental (ecosystem) protection approaches. Thus, institutions that apply the recommended approach derived from the results of the study will be able to contribute for better free energy source. Researchers will be guided on what should be emphasized by the results to harness a better energy. Their study will help them uncover solar energy data that will be gained from the scheffler reflector. Finally, society those living around the off grid area will be benefited if appropriate installation of scheffler reflector is done.

## CHAPTER TWO

### 2. LITERATURE REVIEW

This chapter provides a review of the literature on scheffler reflector, historical outlook, general application areas and the systematic design of the scheffler reflector. The main purpose of this literature review is to reveal the academic and research areas that related to the topic studied.

#### 2.1 Scheffler reflector

Munir et al. [1] described about the design principle and construction details of an 8m<sup>2</sup> surface area Scheffler concentrator and tabulated mathematical calculations to design the scheffler reflector curve and its elliptical frame with respect to equinox by selecting a specific lateral part of a paraboloid. Crossbar equations and their ellipses, arc lengths and their radii are also calculated to form the required lateral section of the paraboloid. Thereafter, the seasonal parabola equations are calculated for two extreme positions of summer and winter in the northern hemisphere.

Daily and seasonal tracking mechanism of the sun's position through a simple mechanism. The design procedure is simple, flexible and does not need any special computational setup. Thus offering a huge potential for application in domestic as well as industrial configurations [2] Jose Ruel as et al. developed and applied a new mathematical model for estimating the intercept factor of a Scheffler-type solar concentrator (STSC) based on the geometric and optical behavior of the concentrator in Cartesian coordinates. In addition, the incorporation of a thermal model of the receptor is performed using numerical examinations to determine the technical feasibility of attaching the STSC to a 3kWe Stirling engine [2]. In experimental set up sterling engine is placed at the focal point, which converts heat energy into electricity.

Mathematical modelling is verified with the help of experimental results. The results allow for the determination of the focal length, which demonstrates that the largest concentration using the STSC with a rim angle of 45<sup>0</sup> is similar to the concentration achieved with a parabolic dish, but the receptor improves the efficiency by 7% compared with parabolic dishes that operate with a lower error of concentration. [3] in the same way, Rupesh J. Patil studied the performance of Scheffler reflector of 8m<sup>2</sup>

with the help of single large diameter drum of 20litre capacity, which serves the dual purpose of absorber tube and storage tank. The performance of Scheffler reflector was analyzed by average power and efficiency in terms of boiling test conducted at Bangalore. The maximum temperature attained by water is 94°C on clear sunny day and ambient temperature varies from 28°C to 31°C. Both dimensional analysis and mathematical modelling was an attempt to correlate dependent and independent variables. Vishal R Dafleet et al(4) designed, developed and analyzed experimentally the performance of 16m<sup>2</sup> scheffler reflectors for 2bar pressure and 110° C temperature. The system was mainly designed for hostel with 500 students at Shivaji University for hot water for bathing and steam for cooking and the Scheffler along with mild steel absorber plate was evaluated in February.

It was observed that radiation varies from 620 W/m<sup>2</sup> to 937 W/m<sup>2</sup> and maximum temperature attained by steam is 107°C. Additionally, the performance of concentrating solar thermal devices using Scheffler technology for water heating and low pressure, temperature steam applications in industries as textiles, dairies, food industry etc[3]. Rupesh J Patil et al carried out work on scheffler reflector for experimental data based modelling to establish relationship in different variables of Scheffler reflector. Scheffler reflector was studied with a typical experimental plan of simultaneous variation of independent variables. Experimental response data was analyzed by formulating the dimensional equations. The models have been formulated mathematically for the local conditions. It was observed that the mathematical models can be successfully used for the computation of dependent terms for a given set of independent terms.

Later, Scheffler reflector has been designed to supply sufficient heat energy to the crematorium by concentrating solar energy. It was assumed that 100kg of wood is required for cremating a single corpse in 1 to 2Hrs if heat loss is optimized to minimum value by effective insulation of combustion chamber. Since calorific value of wood is 19700kJ/kg. The “P” power (in MJ/hr) required to burn completely the body in combustion chamber is determined. From this reflector was designed to cremate a dead body in 2hrs.

S.Kumar et al. [28] has experimentally investigated a 16m<sup>2</sup> scheffler concentrator system and its performance assessments. It is equipped with a polar axis tracking

mechanism to track the sun with its 5 and 4 meter major and minor axis respectively with its concentration ratio of 220. The axis of rotation is congruent with the local altitude. So that the axis of rotation of the reflector and polar axis are parallel to each other. The axis of daily rotation is located exactly in a north–south direction, parallel to Earth's polar axis and runs through the center of gravity of the reflector. That way the reflector always maintains its gravitational equilibrium and the mechanical tracking device does not need to be driven by much force to rotate it synchronized with the sun.

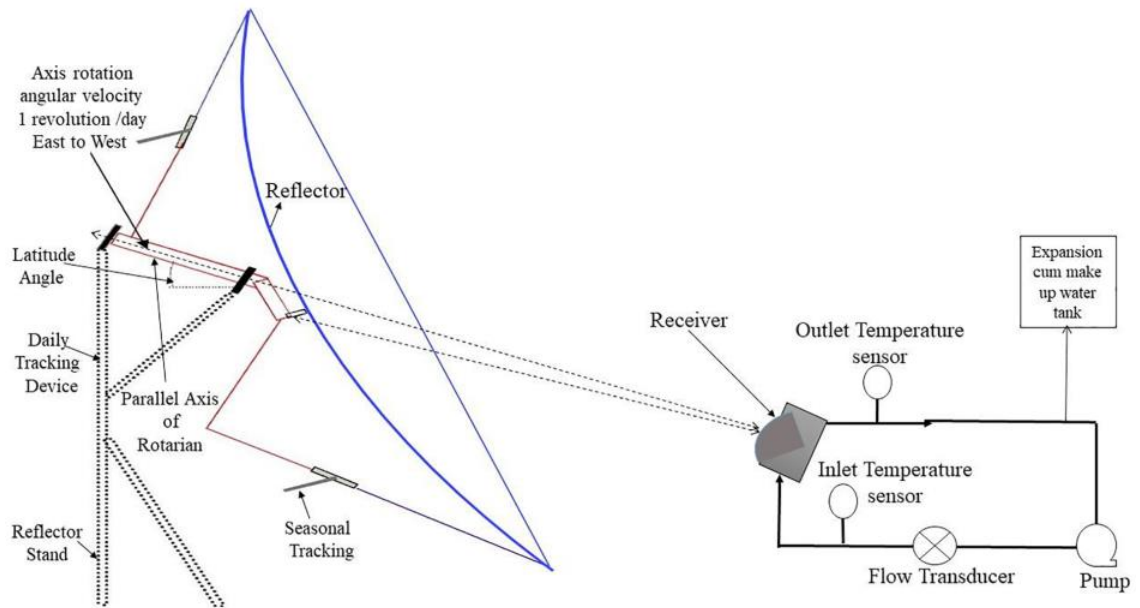


Figure 2. 1 Schematic diagram of the Scheffler concentrator system [28]

The focus is located on the axis of rotation and avoids it from moving when the reflector rotates. During the day, the concentrated light will only rotate around its own center, but not move sideways in any direction and that way the focus stays fixed. The seasonal tracking consists of a telescopic clamp and three triangular pivot points at the reflector. The telescopic clamp is manually set once in every three days in order to get the fixed focus in the receiver. The working fluid (water) is supplied to the receiver and gets heated at a certain temperature for various end-use process heat applications. A 16 square meter Scheffler technology tested in Ludhiana (Latitude: 30.9°N; Longitude: 75.85°E), India as shown in figure below.





Figure 2. 2 a Scheffler dish [3]

## 2.2 Scheffler Concentrator for Solar Cooking

As mentioned before, the German scientist Wolfgang Scheffler has devised a parabolic concentrator set-up to harness solar energy using low cost set-up. A concentrating primary reflector tracks the movement of the Sun, focusing sunlight on a fixed place. The focused light is used to heat a very large pot, which can be used for baking breads, heating, steam generation, cooking, and water heating [2].

Design and development of the Scheffler concentrator is to make solar cooking comfortable. Cooking is simple and comfortable as the focus does not have to be moved and it may even be inside a kitchen, while the concentrating reflector has to be in the sun. The concentrator is flexible parabolic concentrator, which rotates around an axis parallel to the earth's axis, to cope with the sun [3]. Additionally the reflector is adjusted to the seasons by tracking it in a simple way [4].

The tracking mechanism can be a combination of electronic and mechanical design, which tracks the sun [28]. Scheffler also can have an automatic tracking mechanism (counter weight driven clockwork) and due to the dish having flexible curvature gave fixed focus and thus offered a solution to both cooking in comforts in shadow of the kitchen and also being automatic with no need to be tracked manually. According to Munir et al [1], a simple photovoltaic device located in the center of the reflector guides

daily tracking and if this technology is not available, mechanical clockwork can be replaced [24].

From the journal survey, Scheffler concentrators have been built in very different sizes: as small as 0.5 square meters and as big as the 50 square meters reflectors, including medium sizes (2, 2.7, 8, 10, 9.7, 10, 12.6, and 16 square meters), While the main construction of the concentrators (apart from the mirror surface) consists of steel. Profiles that are known in making of furniture, water-installation and housing are used. This material is relatively seems cheap and available. For the concentrator surface, various materials like silvered glass mirrors, aluminum sheet, aluminized materials are used [3].

In general, Parabolic Scheffler concentrator has a potential to deliver a high temperature for all types of cooking and steam generations. Their specialty is due to its flexible surface curvature and a fixed focal area. As Rupesh et al [29] investigated in a 2.7 square meters concentrator, maximum temperature in the focus may reach 102°C, and it is possible to boil 22 liters of water per day (with a solar radiation of 700W/m<sup>2</sup>). A 2.7 square meters reflector may lead 1.2 liters of water to boiling point in 10 minutes. A 9.7 square meters reflector may lead 4.5 liters of water to boiling point in 10 minutes. Thus, integration of Scheffler with thermal storage device may give a convenient indoor cooking with or without the presence of radiation [29].

Table 2.1 Summary of literature review

Author	Task performed	methodology	Result obtained	Validation
A. Munir et al.(1)	The principle and construction detail of an 8m <sup>2</sup> Scheffler reflector	Mathematical modeling	The results have proved mathematically that it is possible to construct a concentrator that can provide fixed focus for all the days of the year.	Mathematical modeling

Desireddy Shashidhar Reddy et al.(2)	Developed Design charts for Scheffler reflector using the two parameters that are required to begin the construction of a Scheffler reflector using the design charts are: (a) The aperture area and (b) The focal length of the parabola.	Mathematical design and experimental testing	<p><b>1.</b> For working design of the Scheffler reflector, inclination angle can be varied in a very small window of 42–44.9°.</p> <p><b>2.</b> The general equation of parabola with changing solar declination (seasonal change) has also been proposed</p>	Mathematical modeling experimental testing
José Ruelas et al.	modeled and developed a Scheffler-type solar concentrator coupled with a Stirling engine	- Experimental -modeling	to obtain the quantity and quality of energy required by the 3 kWe Stirling engine, which corresponds to a thermal energy demand of 8423 W with a fluid temperature of 957K	Experimental analysis
S. Kumar et al	Experimentally investigated a 16m <sup>2</sup> scheffler concentrator the effect of various parameters such as -optical efficiency, -heat loss coefficients, -DNI on the performance of the system.	experimental -modeling	<p>Thermal output is 7.2kW at DNI of 720W/m<sup>2</sup></p> <p>-Thermal efficiency with improved heat loss</p> <p>-Thermal efficiency with improved optical efficiency</p>	Experimental testing modeling
Praveen J. Sanga et al	Performance Evaluation of scheffler Concentrator	Experimental	Better Efficiency than other solar concentrators	Experimental testing

## CHAPTER THREE

### 3. METHODS AND MATERIALS

#### 3.1 Study location

Jimma city found at about 347 km to the southwest of the capital city of Ethiopia, Addis Ababa. Specifically, it is located at geographical coordinates  $7.6739^{\circ}$  N-latitude,  $36.8358^{\circ}$  E-longitude and at an altitude of 1780m above mean sea level with a total population based on central statistical agency of Ethiopia (CSA) is about 184,925 in 2017 GC. (Sisay, Beyene, & Alemayehu, 2017).

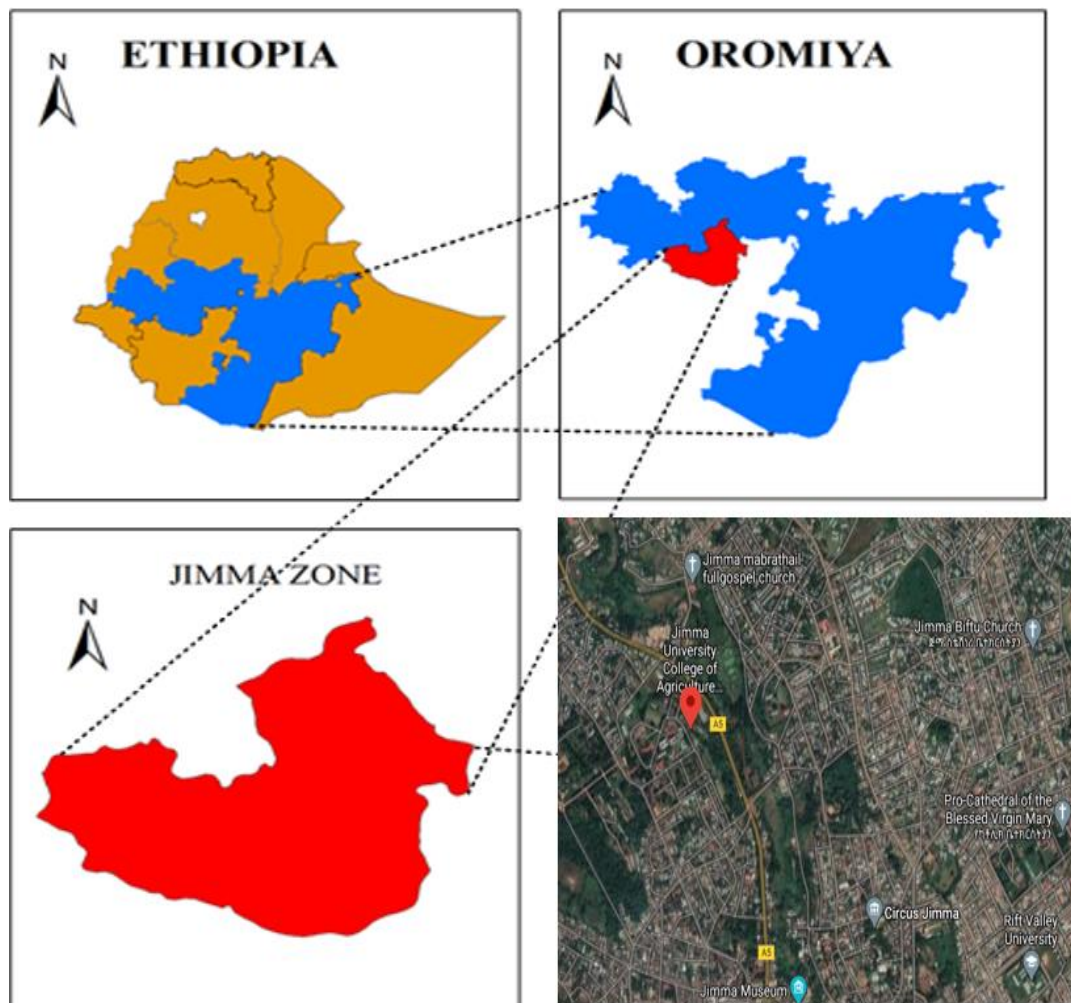


Figure 3. 1 Study location

### 3.2 Methodology

Under methodology, the work passed through a series of steps like, data collection, designation of the research, and simulation of the desired output, to figure out the best reflector's best tracking system.

The present study is to carry out performance assessment of elliptical dish (scheffler) coffee roaster. To achieve the objective of the work, surveying the literature from the related work and understanding the working mechanism of scheffler reflector referring from journals, books and other articles. To analyze the available solar potential of the study area, direct solar radiation measurement and system thermal calculation is done.

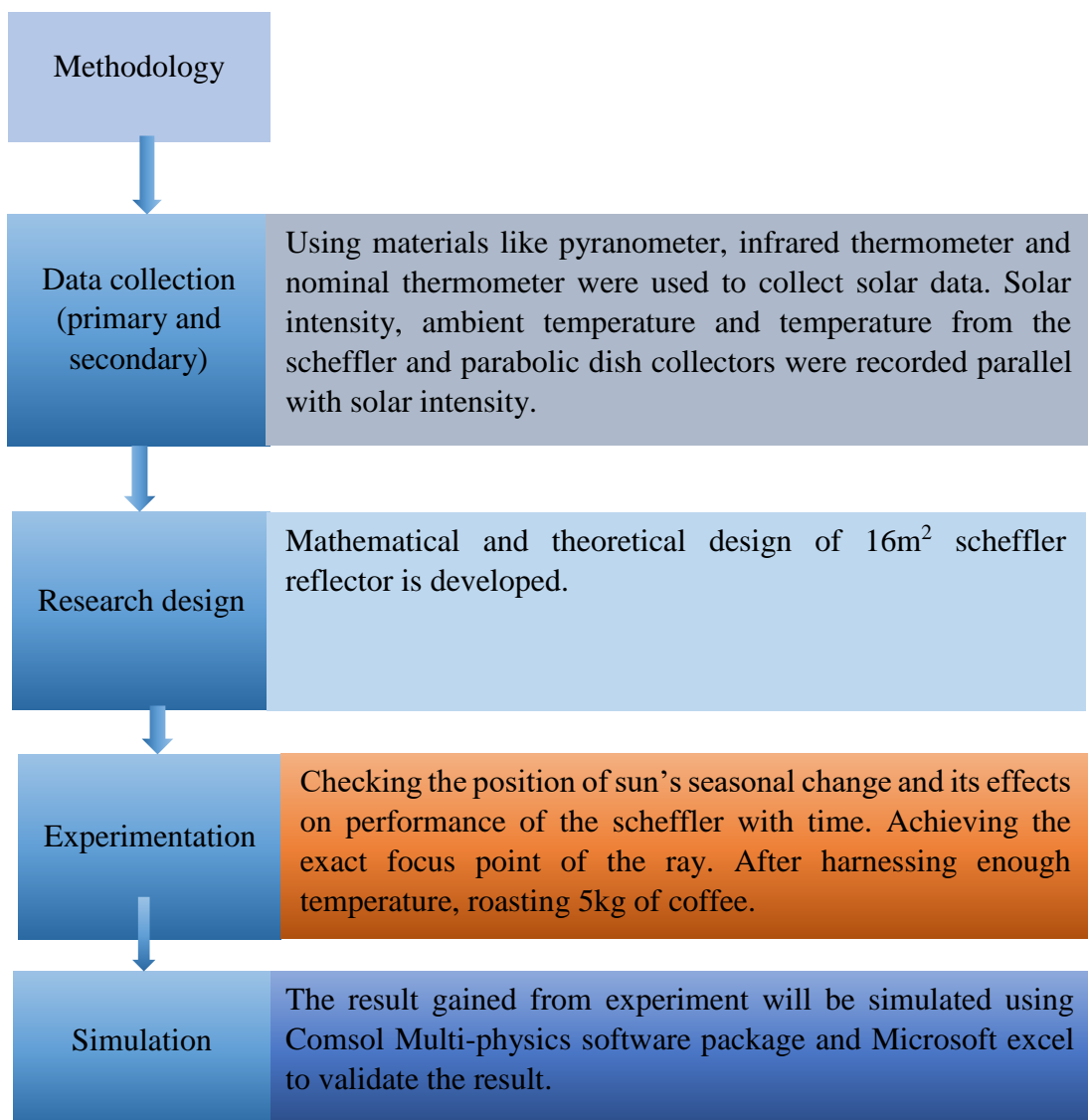


Figure 3. 2 summary of methodology

Scheffler reflector is a lateral portion of the paraboloid, which provides fixed focus and shadow less concentration throughout the year. The lateral portion is obtained by the intersection of an inclined plane with the paraboloid. The side view of inclined sectional plane and paraboloid are represented by a line ( $E_1E_2$ ) and a parabola in a 2D plane as shown in Figure 3.3. It should be noted that the present analysis has been carried out assuming the collector axis (Y-axis) is pointing towards the sun when solar declination angle  $\delta=0^\circ$ . The hourly tracking axis of the Scheffler reflector of focal length ' $f$ ' passes through the focus and the point P ( $2f, f$ ). Positive X axis points towards north in northern hemisphere and south in southern hemisphere and Z axis lies in east-west direction in Figure 3.3. The inclined line  $E_1E_2$  has to be chosen such that the reflector is balanced with respect to pivot point P so that a nominal force is required for tracking the sun.

For the assessment of the scheffler reflector (elliptical dish) which has been installed for the purpose of coffee roasting, this report has passed through series of processes to identify its technical problems why it could not concentrate the ray coming from the sun. For instance, different solar data has been gathered. To collect those data different scientific materials are used. To list some of them, infrared thermometer, pyranometer (with multi-meter which converts incoming beam radiation to millivolts) and nominal thermometer. Later the millivolts displayed on multi-meter manually converted in to watts per square meter ( $W/m^2$ ).

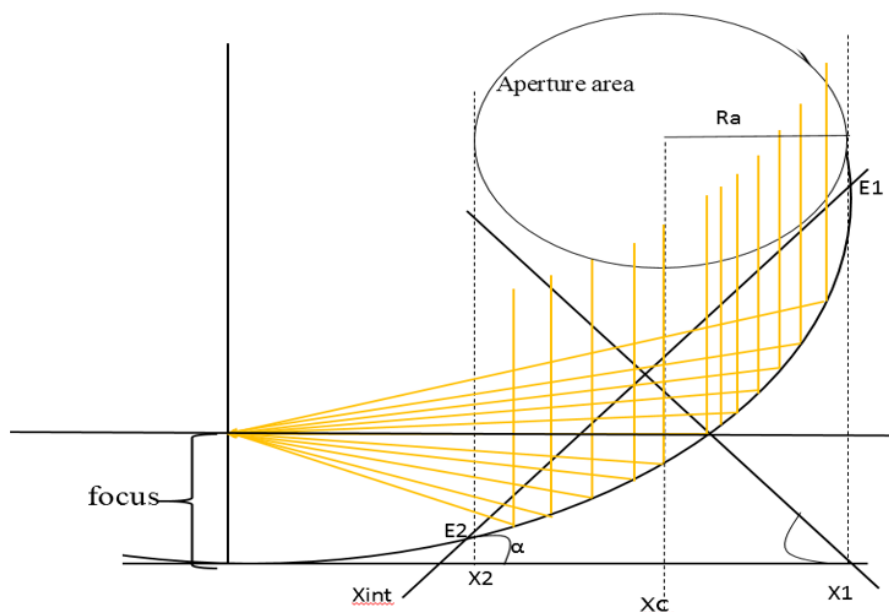


Figure 3.3 scheffler reflector.

The contour created because of the intersection of an inclined section plane and a paraboloid is an ellipse. It shows the elliptical rim of the Scheffler reflector, which appears as a circle (aperture) in the top view. The details are shown in Figure 3.4. A parabola of focal length  $f$  with its vertex at origin and axis aligned with y-axis is written in the following form

$$x^2 = 4fy \quad (1)$$

The slope intercept of the line  $E_1E_2$  is given as

$$y = (x - x_{int})\tan\alpha \quad (2)$$

If the line  $E_1E_2$  and parabola intersect at points  $E_1(x_1, y_1)$  and  $E_2(x_2, y_2)$  the radius of the aperture of scheffler which same as semi-minor axis of its elliptical ring which is given by

$$Ra = \frac{x_1 - x_2}{2} \quad (3)$$

By substituting eq. (3.2) in eq. (3.1)

$$x^2 = 4f(x - x_{int})\tan\alpha \quad (4)$$

$$x^2 - (4f\tan\alpha)x + 4fx_{int}\tan\alpha = 0 \quad (5)$$

The roots of the above equations are:

$$x_1 = \frac{4f\tan\alpha + \sqrt{(4f\tan\alpha)^2 - 16x_{int}\tan\alpha}}{2} \quad (6)$$

$$x_2 = \frac{4f\tan\alpha - \sqrt{(4f\tan\alpha)^2 - 16x_{int}\tan\alpha}}{2} \quad (7)$$

The x-coordinate of the Centre of the aperture is given by

$$x_c = \frac{x_1 - x_2}{2} \quad (8)$$

From equations (2), (3) and (4)

$$x_c = 2f\tan\alpha \quad (9)$$

Then from figure1,  $X_1$  and  $X_2$  can be represented by

$$2f\tan\alpha + Ra \quad (10)$$

$$2f\tan\alpha - Ra \quad (11)$$

The elliptical dish has to be balanced at  $P(2f, f)$  while rotation for hourly tracking of sun is on progress. This helps to reduce the rotational force (torque) required to rotate the dish. Thus, length  $E_1P$  and  $PE_2$  along the parabola must be equal. Reddy et al [25] found that  $\alpha$  should have values within the limits of  $42^\circ$  and  $44.9^\circ$ . The upper limit is fixed to  $44.9^\circ$  due to geometrical constraints whereas below  $41^\circ$  will make  $x_{int}$  negative casting

absorber's shadow on the reflector. Since the aim of this report is not only to clarify the design of scheffler reflector, the portion of this document stands on performance assessment of the elliptical dish coffee roaster which is installed in Jimma University college of Agriculture and Veterinary Medicine compound. During the assessment, relevant data has been recorded.

### 3.3 Mathematical development of scheffler reflector

From its design concepts, scheffler reflector is a side view of a parabola. A concentrator is primary reflector, which tracks the movement of the Sun, focusing sunlight on a fixed place. The focused light is used to heat the absorber, which roasts coffee bean.

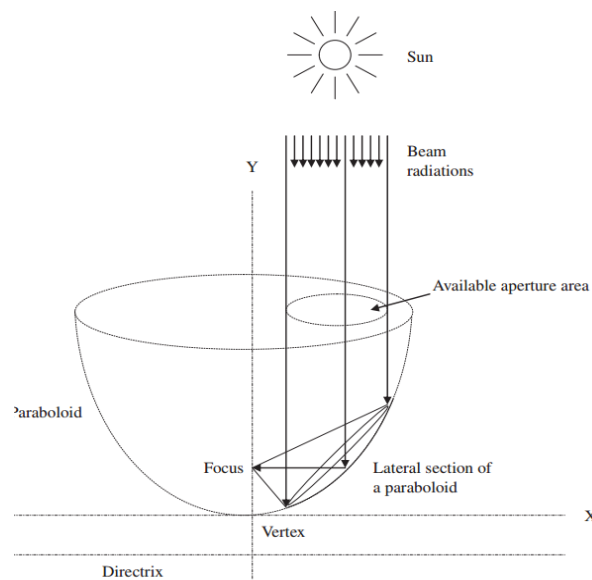


Figure 3. 4 Section of Scheffler reflector in a paraboloid [1]

Unlike a conventional paraboloid concentrator, the Scheffler fixed focus concentrator is a lateral part of a paraboloid as shown in figure above. While designing a parabola curve for the Scheffler reflector, all calculations are done with respect to equinox (zero solar declination). In order to calculate the equation of the parabola curve, the calculations are made by considering the side view of the paraboloid. In this way, the paraboloid and reflector frame are drawn in the form of a parabola curve and straight line respectively. We can write from the basic parabola equations with its axis passing through the y-axis as described in the following section.

$$P(x) = m_p x^2 + c_p \quad (12)$$

Where  $m_p$  is the slope of parabola and  $C_p$  is the y-intercept of the parabola.



Taking first derivative of Eq. (3.12) for the slope of parabola

$$P'(x) = 2m_p x \quad (13)$$

### 3.3.1 Procedure to Design the Concentrator Parabola

The following are the basic steps in the design of parabola [30]

- i. Selection of x-coordinate of point P<sub>n</sub> (x<sub>p</sub>) in order to get a reasonable distance to the focal point; calculation of y-coordinate of point P<sub>n</sub> (y<sub>p</sub>) and slope m<sub>p</sub> with the help of Equations (3.12) and (3.13).
- ii. Selection of XE<sub>1</sub> and XE<sub>2</sub> figure 3.5 in order to get a surface of approximately 16m<sup>2</sup> and a balanced collector; calculation of YE<sub>1</sub>, YE<sub>2</sub> and angle of the line joining the points E<sub>1</sub> and E<sub>2</sub>.
- iii. Check if the two aims are roughly reached (calculation of surface area right and left of P<sub>m</sub> and check their difference for balancing and their sum for collector surface); otherwise adapt a new set of P<sub>n</sub>, E<sub>1</sub> and E<sub>2</sub>.
- iv. Calculation of semi-major and semi-minor axis of the concentrator frame.

For a surface area of 16m<sup>2</sup>, the x-coordinate of the point P<sub>n</sub> is taken as 5.74. (All calculations are based on the point P<sub>n</sub> with x-coordinate as 5.74. This coordinate defines the distance of this point to the focal point, which is also an indicator to the average distance of the reflector surface to the focal point. A value is taken that keeps this distance small, but still leaves some space between the inner collector edge and the focal point in order to avoid shading from the building that usually exists around the focal point.

Therefore, collectors with a higher surface area will generally have a point P<sub>n</sub> with a higher x-coordinate. The first derivative of Equation (3.12) at this point is equal to the slope at the point. The tangent cuts this point P<sub>n</sub> at an angle of 45° with x-axis (directrix), so we can write:

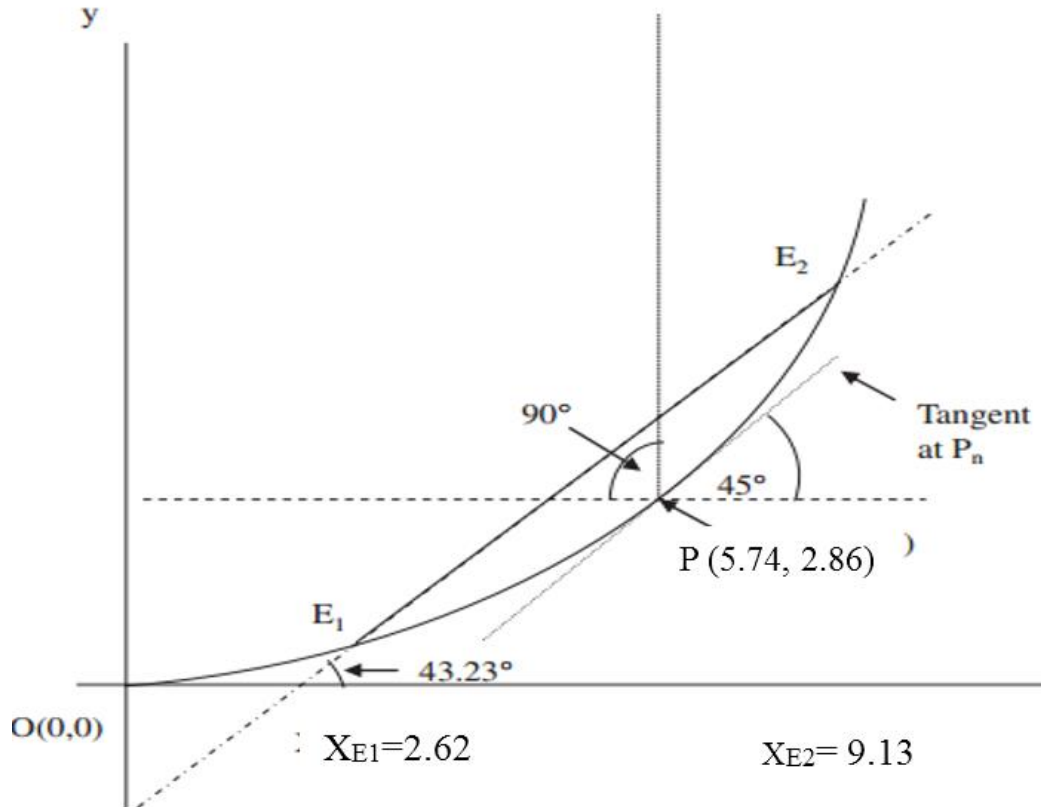


Figure 3. 5. Description of parabola of a Scheffler reflector.

$$P(5.74) = \tan 45^\circ$$

$$P(5.74) = 1$$

According to the definition of parabola, the coordinates at point  $P_n$  are given as:

$$P(5.74) = 1/2 * (5.74)$$

$$P(5.74) = 2.86$$

By using equation (3.2) the values of  $m_p$  are calculated as

$$P'(m) = 2m_p, p'(x) = 1$$

$$m_p = \frac{1}{2 * 5.74} = 0.08$$

Again for equation (3.1)

$$P(x) = p'(5.74) = 2.86$$

$$C_p = mp^2 + cp = 0$$

The parabola equation for equinox is given as:

$$P(x) = 0.08x^2 \quad (14)$$

In order to construct a balanced reflector, two points  $XE_1$  and  $XE_2$  are calculated on a graph paper as 2.62 and 9.13. The reason of selecting these points is to construct a

balanced parabola in order to rotate the reflector with a nominal force. In this way, the line joining these two points  $E_1$  and  $E_2$  of the parabola curve represents the cutting section of the elliptical frame of the Scheffler reflector. This line  $E_1E_2$  is not parallel to the tangent at point  $P_n$  (which makes  $45^\circ$  angle with x-axis) but makes a  $43.23^\circ$  angle as shown in Figure 3.5. The structure is equilibrated and needs a little force to move the reflector.

As we can see in Figure above, the general equation of this straight line is given by:

$$G(x) = m_g x + C_g \quad (15)$$

Where  $m_g$  is the slope of the line and  $c_g$  is the y-intercept of the line

Differentiating equation with respect to x-gives

$$G'(x) = m_g$$

$$m_g = \tan 43.23$$

$$G'(x) = \tan 43.23$$

$$G'(x) = 0.94$$

The coordinate x of point  $E_1$  ( $x_{E_1}$ ) is selected to be 2.64 and the coordinate y is calculated to be 0.56 by using Eq. (3.15). By substituting the values of x, y and  $m_g$  in Eq. (3.15), the y-intercept ( $C_g$ ) is calculated to be -1.92 and the equation of the straight line becomes:

$$G'(x) = 0.94x - 1.92 \quad (16)$$

The coordinate x of point  $E_2$  ( $x_{E_2}$ ) is calculated by comparing and solving Eqs.(1) and (4), the general form of a quadratic equation is as follows i.e.

$$P(x) = G(x)$$

Which gives the general form of a quadratic equation,

$$x^2 - \left(\frac{m_g}{m_p}\right)x + \left[\left(\frac{c_p}{m_p}\right) - \left(\frac{c_g}{m_p}\right)\right] \quad (17)$$

Through solving Eq. (3.17) with the help of a quadratic formula to get two points of intersection ( $x_{E_1}$  and  $x_{E_2}$ ) of the parabola curve and straight line, we get:

$$X_{E1} = \frac{m_g}{2m_p} + \left[ \left( \frac{m_g}{2m_p} \right)^2 - \left( \frac{c_p - c_g}{m_p} \right) \right]^{\frac{1}{2}} \quad (17a)$$

$$X_{E2} = \frac{m_g}{2m_p} - \left[ \left( \frac{m_g}{2m_p} \right)^2 - \left( \frac{c_p - c_g}{m_p} \right) \right]^{\frac{1}{2}} \quad (17b)$$

By equating the two equations of lines (parabola and straight lines), the point of intersection for the two graph lines can be calculated.

$$0.08x^2 = 0.94x - 1.92$$

Rearranging the equation,

$$x^2 - 11.75x + 24 = 0 \quad (18)$$

The two roots are 9.13 and 2.62.

The straight line cutting the curve represents a cutting plane of an ellipse with axes ratio  $a/b = \cos\alpha$ , where “a” and “b” are the semi-minor axis and semi-major axis respectively. For a given paraboloid, the cutting section of the lateral part will make an ellipse and its projection on the ground (horizontal plane) will make a circle. Therefore, the semi-minor axis of the ellipse and radius of projection on the ground will become the same. The projection of this ellipse on the horizontal plane (xz-plane) is a circle with a diameter of  $2a$ . The general equation for the diameter of circle (2a) is calculated for a Scheffler reflector by subtracting Eq. (3.17b) from Eq. (3.17a) and is given by:

$$2a = 2 \left[ \left( \frac{m_g}{2m_p} \right) - \left( \frac{c_p - c_g}{m_p} \right) \right]^{\frac{1}{2}} \quad (19)$$

The semi-minor axis of the ellipse is 2.74m and semi major axis of the reflector is calculated to be 3.75m by dividing with axes ratio ( $\cos 43.23^\circ$ ).

### 3.4 Distribution of crossbars on the reflector frame

For the construction of the Scheffler reflector, it is necessary to know the exact position of the crossbars on the reflector frame. The frame of the Scheffler reflector is elliptical in shape and this can easily be calculated by using the equation of ellipse, which is given below:

$$\left( \frac{x}{b} \right)^2 + \left( \frac{y}{a} \right)^2 = 1 \quad (20)$$

Where ‘a’ is the semi-minor axis of the ellipse, b is the semi major axis of the ellipse. In order to locate any point “ $y_n$ ” with respect to “ $x_n$ ” on the elliptical frame, Eq. (10) can be written as:

$$yn = \cos 43.23[b^2 - x^2]^{0.5} \quad (21)$$

Equation above is used to calculate the position of crossbars on the elliptical frame of the Scheffler reflector. A number of points can be taken but not more than seven to nine crossbars are sufficient to make the required section of the paraboloid for a 16m<sup>2</sup> Scheffler reflector.

### 3.4.1 Calculation of equations for crossbars ellipses

The cutting planes of the crossbars are perpendicular to the cutting plane of the reflector frame and are shown in the form of seven straight lines (q<sub>1</sub>–q<sub>7</sub>) as shown in Figure 3.7. The inclination angle of the cutting plane of crossbars is found to be -46.77<sup>0</sup> by subtracting the angle of the cutting plane of the reflector frame from 90<sup>0</sup>. These cutting lines are ellipses with axes ratio (a<sub>q</sub>/b<sub>q</sub>) = cos 46.77. Starting from the middle crossbar (q<sub>4</sub>, passing through Pc), we take from the basic equation of the line and it is given as:

$$q_4(x) = mq_4x + cq_4 \quad (22)$$

Slope of the middle crossbar is calculated as:

$$mq_4 = \tan(-46.77) = -1.06$$

The x-coordinate of the point of intersection (Cf) of the middle crossbar and the reflector frame is the central point of xE<sub>1</sub> and xE<sub>2</sub>. The y-coordinate is calculated by substituting this value of x in Eq. (3.16) and is given as follows:

$$q_4(5.43) = 3.2$$

Substituting the values of mq<sub>4</sub>, q<sub>4</sub>(x) and x in Eq. (3.22), the y-intercept (C<sub>q4</sub>) for the middle crossbar is calculated and the equation of the middle crossbar (q<sub>4</sub>) for 16m<sup>2</sup> surface area of the Scheffler reflector is given as:

$$q_4(x) = -1.06x + 8.94 \quad (23)$$

It is evident from Fig. 3.7 that the slopes for all cutting crossbars are the same as these are perpendicular on the same cutting plane of the Scheffler frame. As the crossbars are equally distributed (from the center of the reflector frame), so the difference between the two successive y-intercepts can be set according the requirement and based on size facets of the glass mirror attached. In this case, 0.7 is taken.

The equations for the 4th, 5th and 6th crossbars are calculated by adding 0.70, 2(0.70) and 3(0.70) in the y-intercepts values of Eq. (3.23) respectively. Similarly, the equations for 3rd, 2nd and 1st crossbars are calculated by subtracting 0.70, 2(0.70) and 3(0.70) from the y-intercepts values of Eq. (3.23) respectively.

The equations for all crossbars can be generalized as  $q_n(x) = m_q x + C_{qn}$ . Similarly, for a semi-minor axis ( $a_{qn}$ ) of any crossbar ellipse, Eq. (3.19) can be modified for crossbars and the reflector frame and is generalized as:

$$a_n = \left[ \left( \frac{m_{qn}}{2m_p} \right)^2 - \frac{c_p - c_{qn}}{m_p} \right]^{\frac{1}{2}} \quad (24)$$

Where subscript “n” represents the number of crossbars

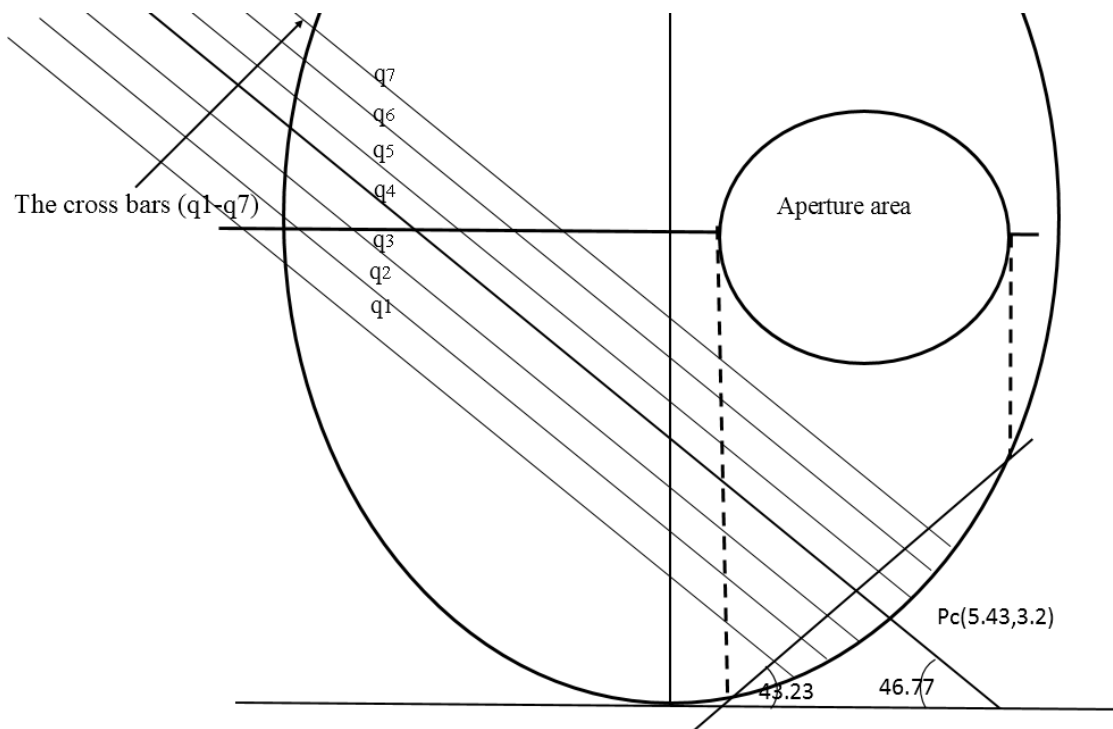


Figure 3. 6 Description of the Scheffler reflector and crossbars on parabola curve

### 3.4.2 Calculation of depths and arc lengths for different crossbars

After the calculation of equations for different crossbars, the depths and lengths of arcs for different crossbars are calculated for the construction of the Scheffler concentrator [1]. The depth of reflector for the nth crossbar ( $D_n$ ) is calculated from the following formula and is explained in Figure 3.8 shown below [1].

Crossbar n	y-intercept Cqn (m)	Equation of cutting section cross bars on xy plane	Semi-minor axis aqn (m)	Semi-major axis bqn (m)
1	6.84	$q_{4(x)} = -1.06x + 6.84$	7.06	10.31
2	7.54	$q_{4(x)} = -1.06x + 7.54$	7.35	10.73
3	8.24	$q_{4(x)} = -1.06x + 8.24$	7.62	11.13
4	8.94	$q_{4(x)} = -1.06x + 8.94$	7.89	11.52
5	9.64	$q_{4(x)} = -1.06x + 9.64$	8.15	11.89
6	10.34	$q_{4(x)} = -1.06x + 10.34$	8.39	12.26
7	11.04	$q_{4(x)} = -1.06x + 11.04$	8.64	12.61

Table 3. 1 Equations, semi-minor axis and semi-major axis of different crossbars.

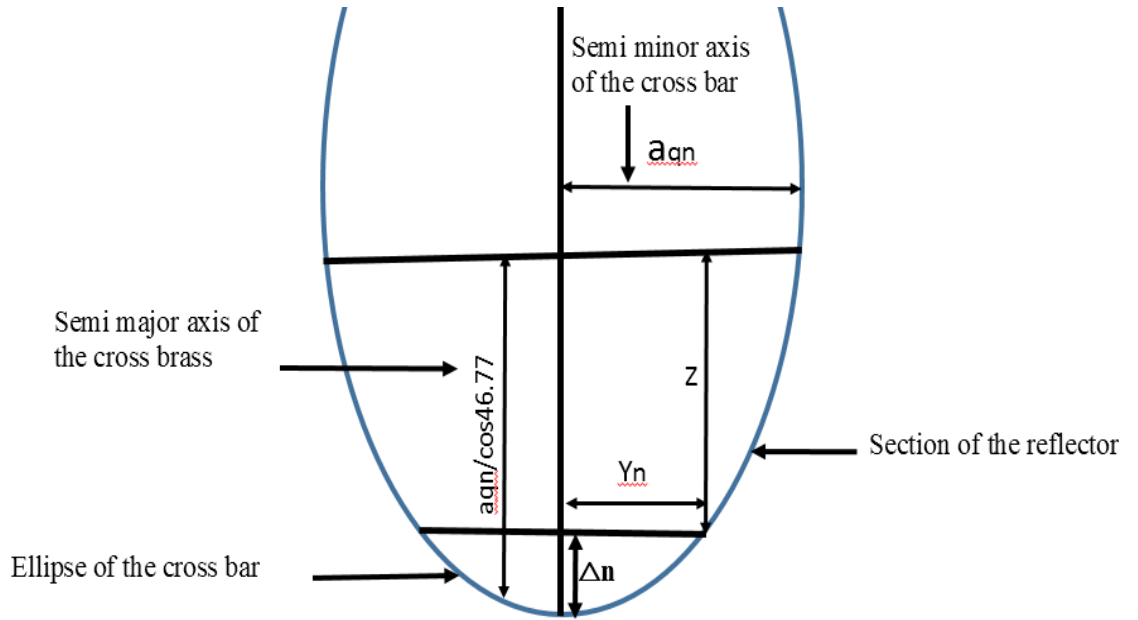


Figure 3. 7 Ellipse of the crossbar for the Scheffler concentrator

$$\Delta n = \frac{aqn}{\cos 46.77} - Z \quad (25)$$

$$Z = \frac{((aqn)^2 - (yn)^2)^{\frac{1}{2}}}{\cos 46.77}$$

From basic formula ellipse by substituting value of z in equation 3.15 we get

$$\Delta n = \frac{[aqn - ((aqn)^2 - (yn)^2)^{\frac{1}{2}}]}{\cos 46.77} - Z \quad (26)$$

We can see that all of the crossbars are the parts of the ellipses that differ slightly from the circle segment.

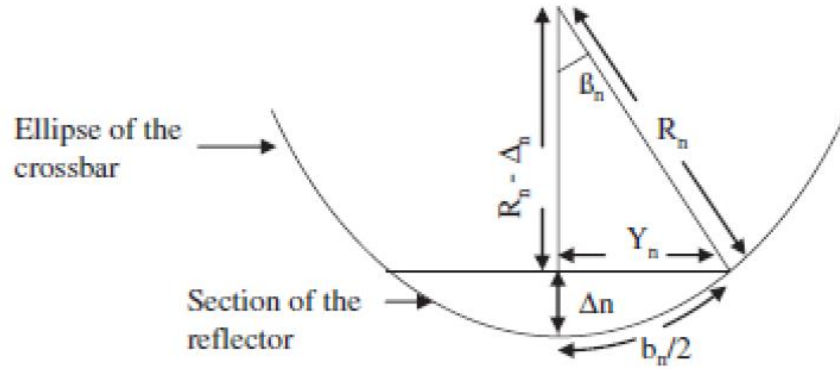


Figure 3. 8 Radius, depth and arc length details for the nth crossbar [3]

For the solar concentrator optics, different approximations are valid to concentrate energy cheaply rather than to form a precise image [17]. As the small segments are used for large ellipses, these small elliptical segments are taken as the parts of circle segments. In this case, since it is along the crossbar, a small placement deviation also means a small angle deviation. For an nth crossbar, radius ( $R_n$ ), depth ( $\Delta_n$ ), arc length ( $b_n$ ) and angle made with half arc length ( $\beta_n$ ) are shown in Figure 3.8 shown.

It is evident from Figure 3.8

$$(R_n)^2 = (R_n - \Delta_n)^2 + (y_n)^2$$

Simplifying the above equation,

$$R_n = \frac{(\Delta_n)^2 + (y_n)^2}{2\Delta_n} \quad (27)$$

It is clear that from Figure 3.6,

$$\beta_n = (\sin)^{-1}(Y_n/R_n) \quad (28)$$

And

$$\frac{b_n}{2} = R_n \left( \frac{2\pi\beta}{360^\circ} \right) \quad (29)$$

In this manner radius ( $R$ ), depth ( $\Delta$ ), arc length ( $b$ ) and angle made with half arc length ( $\beta$ ) of the all the cross bars are calculated by using the equations (27)– (29).

### 3.5 Fixed focus tracking

Elliptical dish is a fixed focus tracking [27]. The present crossbar design is compatible with the unique seasonal tracking mechanism employed in Scheffler reflector,



originally proposed by the German engineer Wolf Gang Scheffler, to achieve stationary focal point throughout the year. The tracking mechanism is briefly explained with the help of schematic, shown in Figure 3.10. The reflector is attached to a shaft along north-south direction at point P with a pivot joint. It rotates for hourly tracking of the sun from sunrise to sunset. It rotates with a constant speed of 1rev/day and is inclined at an angle  $\phi$ , which is the latitude angle of the installation site. This can be automated with the help of a controller and a DC motor powered by a mini-solar panel. It should be noted that the reflector has to be reset to its initial position for tracking the sun next day.

Two telescopic clamps with locks are provided at the top and bottom of the reflector and are joined to E1 and E2 using pivot joints as shown in Fig. 3.10. When the position of the sun (solar declination  $\delta$ ) in sky shifts in a north-south direction with the change in season, the sunrays do not focus at F. In order to refocus solar radiations back at F, the two telescopic clamps are unlocked and the parabola is manually tilted towards the sun's new position. Once the light gets refocused at F, the bottom telescopic clamp is locked. After that, the top telescopic clamp connected to E1 is to be manually pushed or pulled to flex the Scheffler reflector profile until a minimum spot size (a sign of proper concentration) is achieved at the focal plane. The top clamp is then locked and Scheffler reflector is ready for the use. This adjustment can be performed once a week, or less frequently near the solstices, to avoid significant deviation of the spot from focus. This will ensure proper utilization of the installed reflector. The pushing and pulling action of top telescopic clamp causes elongation or compression of the major axis of the elliptical rim with corresponding contraction or elongation of the minor axis, as shown in. When E1E2 (major axis of the elliptical rim) is elongated, the parabolic support moves closer to the inclined plane with a reduced curvature. Each crossbar experiences contraction from two ends at the elliptical rim. This will result in a reduction of overall curvature of the Scheffler reflector.

It is evident that the diameter of aperture circle is equal to the minor axis of the elliptical rim. With elongation of the major axis and subsequent contraction in minor axis, aperture area reduces whereas with contraction of the major axis and subsequent expansion in minor axis, aperture area increases. It is worth mentioning here that telescopic arrangement employed for seasonal adjustment causes a change in curvature of the crossbar as well as that in the curvature of parabolic support. It should be noted that the Scheffler reflector is designed for equinox. The elongation and contraction of

E1E2 changes the focal length of the Scheffler parabolic support without altering the spatial coordinates of focal point **F** and pivot point **P**. Hence, the distance between **F** and **P** remain twice the focal length at the equinox.

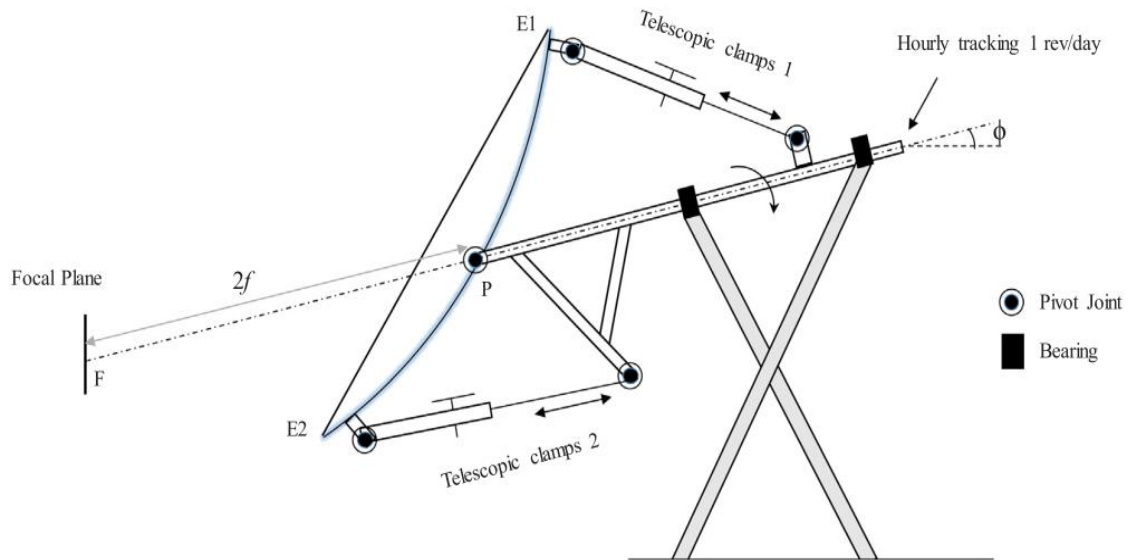


Figure 3. 9 Hourly and seasonal tracking mechanism for Scheffler reflector [25]

The sun gives us the impression of movement because the earth is revolving under our feet. One way to stop moving while rotating is to locate our self in the center or axis of the rotation, the same way, the hot focus of the Scheffler concentrator can be kept at a fixed place in the axis of rotation of the reflector giving maximum convenience for utilization of solar energy [10]. For daily tracking, these reflectors rotate along an axis parallel to polar axis with an angular velocity of one revolution per day to counterbalance the effect of daily earth rotation. The daily tracking is accomplished with the help of a small self-tracking Photovoltaic system or clockwork operated by gravity, which provide angular velocity at one revolution per day.

### 3.6 Moving with the Sun

Just as the earth spins around an axis through the North Pole and the South Pole, the Scheffler Reflector spins around an axis parallel to that, just in the opposite direction. (To counteract the earth's rotation), this is called polar mounting or mounting on a polar axis. The speed is one revolution per day, or, better, half a revolution in half a day, since we do not use it at night. In this way, the concentrator keeps facing the sun in a constant manner [35].

For practical reasons, the shape of the reflector should be such that the hot focus is outside of the reflector, either on the north side or on the south side. This way the hot focus can be even inside a building while the concentrator remains outside. The beam radiation has to be always parallel to the y-axis. Note that in moving with the sun there is a change in the aperture area, the focus F and the center of the Scheffler concentrator (black dot) remain stationary.

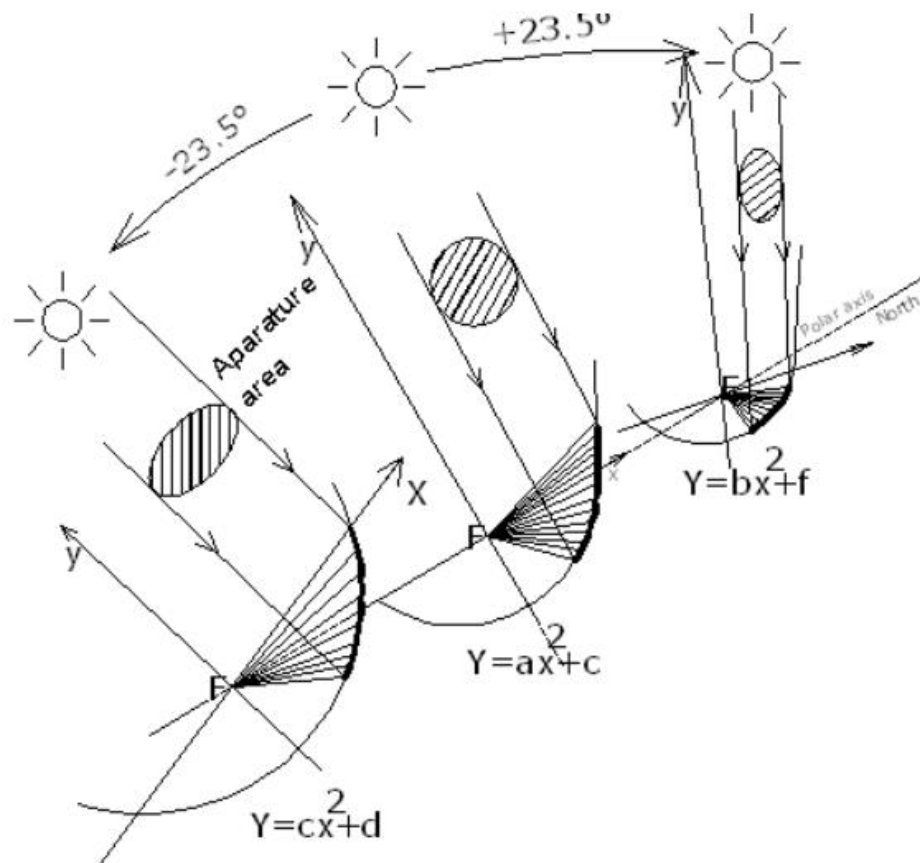


Figure 3. 10 Parabolas focusing the sunlight at a fixed focus by moving with the sun

### 3.7 Coffee roasting and its thermodynamic approach

Roasting coffee is a thermodynamic process in which the application of heat and the resulting uptake of heat by the bean directly affects final flavor. The condition under which heat is applied is affected by environmental factors, including internal volume of the roaster, humidity, barometric pressure, and ambient temperature. The ability of the bean to take on heat and the rate at which the absorbed heat dissipates throughout the bean is a function of its physical state, including percentage moisture, density, and bean size. The chemical changes taking place at any instant in the process depend upon the amount of heat already taken on, the amount of heat available in the immediate environment, the ability of the mass of beans to conduct heat, and the reactions that

have already taken place or are in the process of taking place. The roaster technician adjusts the flame based upon knowledge of the roasting process, observations of the processes taking place, and experience. [18][19]

In developing an understanding of coffee roasting, it is useful to examine the process from a thermodynamic perspective (where the main issues are heat and mass transfer) and from a flavor perspective, (the chemical changes that take place as a result of heat application).

### **3.7.1 Roasting process**

Thermodynamics is the study of energy, its transformations, and its relationship to the properties of matter. In visualizing thermodynamic models, it is useful to define the system under consideration and its boundaries. The system is loosely defined as that which inherently resists change. In this case, the system is defined as the mass of coffee being roasted. Heat transfer occurs from the roasting environment into the coffee across a boundary of zero thickness. The energy in the environment shapes the heat transfer across the boundary of the system. When the heat transfer is flowing from the environment into the system, it is called “endothermic,” heat absorbing; when heat is moving the opposite direction, from the system into the environment, it is referred to as “exothermic.”

The degree to which the system is able to be heated or is resistant to heat is called conductivity. The rate at which heat is transferred from the environment to the system depends on the amount of thermal energy present in the environment and how quickly the system is able to conduct the heat (heat capacity). In the case of coffee roasting, the heat initially moves from the roasting environment into the green bean, referred to as an endothermic reaction. As certain processes take place within the bean, the process gradually becomes more exothermic, releasing heat into the environment. The craft of roasting is based on anticipating these changes and making necessary adjustments. This process for roasted coffee is summarized in the diagram below [20].

When considering classic thermodynamic models, one assumes that heat originating in the environment is crossing a defined boundary into a system (endothermic) or from the system into the environment (exothermic). The system is most easily regarded as a group of rigid spheres with no mass transfer (only energy transfer) and conductivity that does not change. However, as can be seen from the diagram, during the roasting

process the state of the system undergoes changes in terms of both mass transfer and direction of heat movement across the boundary. This necessitates the breaking up of the roasting process into stages that reflect the changes in conductivity, mass, and direction of heat transfer undergone by the system.

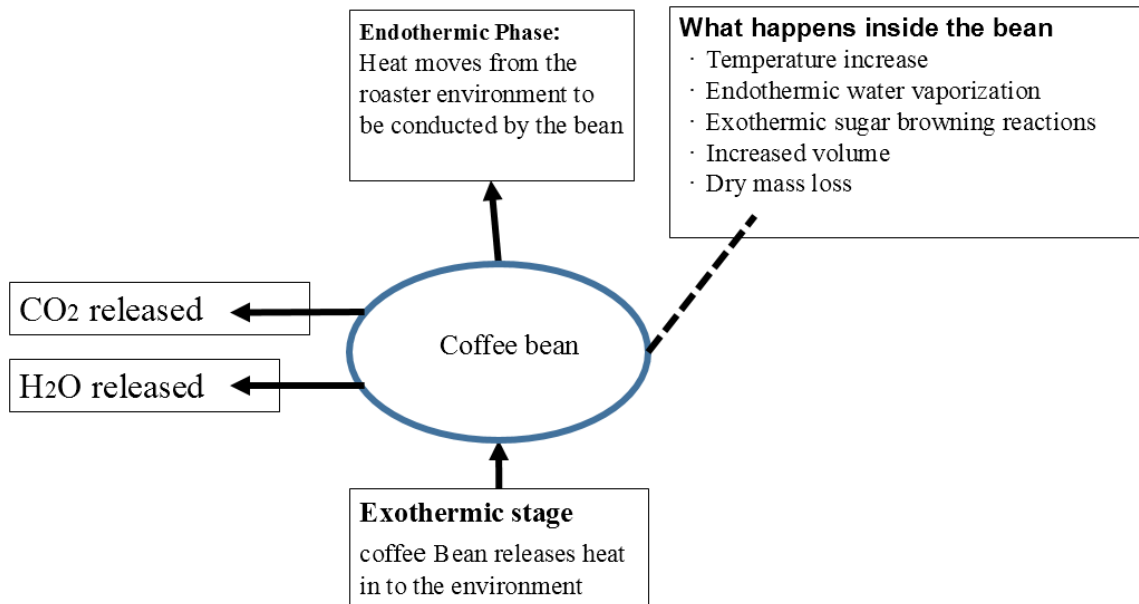


Figure 3. 11 process of roasting coffee

In considering these changes, it is important to review the Second Law of Thermodynamics. Briefly, this states that a thermodynamic driving force (heat, in this case) flows in one direction, from a system or environment that is hot to a system or environment that is cooler. When the temperature difference between two entities is large, the rate of change of temperatures is greater than when the difference is less. Heat is energy in transition and not a property of either the system or the environment. These phenomena are especially observable in coffee roasting, which utilizes large amounts of thermal energy (measured in Joules). Changes in thermal energy result in changes in temperature. For the temperature of a body to continue to rise, thermal energy must continue to be present or enthalpy (energy loss) will occur.

The first change that occurs within the bean is the heating of the green bean’s surface moisture. Some of this moisture is vaporized (for this reason, this stage is referred to as “the drying stage”), collapsing the first layers of cells while some moisture heats the interior of the bean. The roaster observes this by noting expansion in size and a change in bean color.

The beans themselves influence the rate at which this takes place. The conductivity of the system is a function of the physical state of the green coffee. In washed process coffees, the bean moves from a green or blue green to more of a jade green. Natural process coffees (such most Indonesian or Brazil coffees), which begin as pale yellow, deepen in hue to a golden color. The amount of swelling that takes place is an indication of how quickly the bean is taking on heat. This is partially dependent on the amount of moisture in the bean, which typically varies from 9-12%. Past crop coffees (including Central Americans purchased in the fall or early winter) have less moisture and will not take on heat as quickly. Past crop coffees will not turn as richly green and may even fade slightly in the early stages of roasting. This is an indication that more heat will need to be applied over the entire roast period in order to effect the changes desired. The moisture present in the green bean acts as a heat conductor and if less moisture is present; the bean will be more resistant to roasting. Since it can be assumed that there are also high humidity gradients caused by evaporating water that is moving into the roast gas, the thermal properties between the core and the surface of the bean are reasonably different <sup>3</sup>. At this point, not many observable chemical changes are taking place, but this stage may be important in the development of aroma precursors <sup>4</sup>. It is also important in determining how quickly the absorbed heat will distribute throughout the bean. It is possible to overheat the beans at this stage, burning and charring the outside yet not allowing a gradual enough heat penetration. Conversely, if not enough heat is applied (or, as often happens, if the mass of coffee, the “charge,” to be roasted is too large) the beans will not heat evenly. At this stage, a great deal of the thermal energy in the roaster is required for evaporation<sup>5</sup>, but little of that energy is applied towards roasting reactions. The “drying stage” is a preparatory stage and the amount of time it takes will determine the heat difference between the outside and center of the individual beans.

The expansion that takes place at this stage increases the porosity of the bean. What occurs at this point becomes especially important at the later stages of roast; greater porosity will result in decreasing volumetric heat capacity after moisture has been driven off and, especially, after first crack. Fast-roast techniques expand the bean to a greater degree and such coffees have greater porosity.

With sufficient heating of the bean and the removal of a certain amount of surface moisture, the chemical changes associated with coffee roasting begin (referred to as

“roasting proper” by Dr. Clarke [6] and the coffee moves from gold/yellow into a brown or reddish brown phase. This process begins when the bean temperature is around 160° C. This color change indicates that the sugar browning reactions have begun to take place. These browning reactions (which include Maillard reactions, caramelization, and other reactions) gradually move the thermodynamic process from one of an endothermic reaction (heat absorbing) to an exothermic reaction (heat releasing). The “activation energy” at which the sugars begin exothermic chemical reactions is 175°C [8]. The amount and rate of this reaction is determined by the concentration and type of sugars present in the bean (higher quality coffees have a greater amount of sugar than lower quality coffees; past crop coffees have less sucrose but more glucose) as well as moisture content and ambient heat (the increasing bean temperature). This is one of the most important phases of roasting; the rate of roast and resulting chemical reactions will be established as the result of the amount of heat taken on and the rate of sugar browning reactions.

The change in the internal energy of the system at this stage is the sum of the heat entering the system from the environment and the heat being created by the sugar browning reactions. Like a snowball rolling downhill, the sugar browning reactions develop a momentum of their own and the increase in internal energy depends less and less on the heat in the environment as the roast progresses and more on the heat already taken on, the buildup of pressure within the bean, and the heat released by sugar browning.

Important observations to be made by the roaster at this point are color, color change, color uniformity, and the rate of color change. Excessive temperatures are to be avoided since the bean can only take on heat at a certain rate (this may be reflected by uneven splotching of dark brown/black colors on the bean). If the environment is too hot (or if the beans are allowed to remain in contact with hot metal surfaces within the roaster for too long), the result is carbonization and charring of the bean surfaces. On the other hand, if the environment temperature is too low, the heat within the bean will dissipate, halting the roasting reactions.

Besides color, an important clue to the roaster is the aroma of the coffee as it develops. A sourish green aroma, possibly somewhat like peanuts in natural process coffees, is the first to develop. As the coffee moves from golden to reddish-brown, a sweet-roasty

aroma develops. Finally, the more familiar coffee aromas develop at a temperature of 180-190°C [21]. The smell of burning may indicate carbonization.

In a controlled experiment conducted by Eggers, it was seen that the difference between the core and surface temperature was initially 70° C, while the difference between the core and half the distance to the surface was approximately 10°C [22]. Another observation made by Eggers was of “a small temperature drop suddenly appearing at a roasting time of 200 seconds. At this time, the inner temperature differences are clearly higher in comparison to the outer temperature differences. However, the temperature course drops slightly simultaneously throughout the whole bean. After this unsteady phenomenon temperatures increase more rapidly than before! As an explanation, one can assume a pressure built up in the center of the bean due to evaporating of water starting from the surface towards the central region but proceeding with decreasing velocity because the driving force of heat transfer – the temperature difference to the ambient – is diminishing all the time. So the pressure inside the bean increases until the temperatures overcome the vaporization temperature according to the pressure. Thus, the remaining water in the center of the bean evaporates spontaneously and an endothermic flash creates the slight temperature drop [23].

A further consideration is the influence of air movement within the roaster. This creates a change in pressure and convective heat and removes humidity and gasses and will affect the rate of the process, with greater airflow intensifying the effect of the applied heat. The exothermic reactions climax with first crack. At this point, a great deal of heat is released into the roaster and considerable mass transfer from the roasting beans (in the form of moisture, CO<sub>2</sub>, and other gasses) is taking place. Since the bean has expanded and loses mass during this process, it is considerably less dense and will not resist applied heat as easily. As a result, the batch is more subject to carbonization. The amount of exothermic energy released depends on the location, on the temperature, on the time a certain amount of organic compounds is being processed (reaction rate) and on the reaction enthalpy (heat loss as the result of the reaction).

At the point of first crack, the bean has already absorbed the potential heat energy that will produce the reaction. While the sugar browning reactions are occurring, the system is generating its own heat as well as absorbing heat. The exothermic energies lead to a



further increase of the bean temperature without additional heat applied from the roast gas [23].

In general, the roasting process is a thermodynamic process that involves manipulating the heat of the environment (the roasting chamber) in order to bring about chemical changes within the system (the mass of coffee). The success of the process is due to the final degree of roast, the time of roast, and the processes that have occurred as the result of application of heat. Response of the green beans that make up the system to the changes in heat is due to quality, its density, and moisture content. The physical factors of density and moisture content will change as the roast progresses. Each stage in the roasting process is dependent on the amount of heat already absorbed by the system and the roaster must anticipate the amount of heat that will be required. At all stages there is the possibility of losing the roast (allowing the system to exothermic too much of its heat) or burn, carbonizing and adding undesirable flavors to the roast.



Figure 3. 12 roasting coffee using scheffler reflector

### 3.9 Components and material of Scheffler dish

The key components of Scheffler dish are:

- Reflector dish
- Receiver
- Dish stand
- Tracking System

#### *Summary of material of scheffler reflector*

<b>1.Mirror</b>	
parameter	Specification
Type	Solar grade mirror with low iron content or Aluminum reflector with glass like finish for an outdoor use. Aluminum reflectors should have a proper back support for the precise reflective surface area.
Parameter	Specification
Material	Tempered and toughened Solar grade glass/Glass Infused Aluminum/Aluminum tested for scratches and durability.
Shape	Flat mirror cut in required sizes for different models
Size	All dimensions of a mirror should be less than the diameter of the receiver
Thickness	2-3 mm for Solar Grade Mirror/ 0.5mm for Aluminum Reflector
Reflective Coating	High quality silver back coating
Reflectivity	At least 90%
Design	Cross bar structure consisting of square bars and angle sections to form a shape of parabola with metal channels bolted above the square bars for fixing mirror.
Material	all sections & bars made of Standard mild steel and channels of Aluminum
Shape	Parabolic shape
Thickness of structural components	Various hallow sections have variable thickness.
Fixing of mirrors on Support Structure	On the base structure with the help of industrial adhesive and fasteners after ensuring equinox position of the support structure
<b>2.Receiver</b>	
	The receiver of scheffler dish is placed at the focus of the dish to capture the incident solar radiation and transfer it to the thermal medium used in the system.
Design	Spherical type receiver
Material	Boiler grade Mild Steel / SA516 ASTM1

Size & Thickness	Diameter is based on the kg of coffee to be roasted at the same time rate required as per the process
<b>3.Dish stand</b>	
Parameter	Specification
	The basic framework of the dish stand is a steel structure. The structure is designed to withstand wind speed in operating conditions as well as in parked stage as per the applicable structural design code. The overall system rests on a civil foundation. The rotary support, counter weight and other equipment's like an electric motor for tracking are attached on the Dish stand.
Design	Rectangular/Triangular conical shape steel structure consisting of standard IS (Indian Standards) sections, pipes and angles fixed on a cement concrete column
Material	Mild Steel structure and cement concrete
Strength & Durability	Designed to withstand 160 Km/hr. of wind speed with a life span of 20 years
<b>1. Tracking System</b>	
	Tracking system enables the dish to be focused towards the sun to capture maximum possible direct radiation during the day. It also tracks the sun as it changes its position during the seasons
Parameter	<i>Specification</i>
Mechanism	Automatic mechanism (Microprocessor based/Timer based) for daily tracking and manual mechanism for seasonal tracking in 16m <sup>2</sup> scheffler dish system. Automatic mechanism (Timer based) for daily tracking and Semi-Automatic mechanism with the help of switches for seasonal tracking in 32 m <sup>2</sup> scheffler dish system
Equipment used	<ul style="list-style-type: none"> <li>➤ Standard Electric Motor, Rope with counter weight, Gear box, Chain, Timer and Threaded Bars for timer based daily tracking</li> <li>➤ Set of photo sensors, chains, motors, gears and actuators for microprocessor based daily tracking</li> </ul>

Table 3. 2 Components and its Specification



Figure 3. 13 (a) Tracking mechanism (b) footage and support (c) reflector

### 3.9 Materials

Multiple of materials are used during the data collection was in progress. These materials are Pyranometer and infrared thermometer.

#### 3.9.1 Pyranometer

The SP Lite2 measures incoming solar radiation (sun plus sky radiation) with a photodiode detector. Output from the photodiode is a current, which is converted to voltage by an internal shunt resistor. The SP Lite2 can be used in solar energy applications such as plant growth, thermal convection and evapotranspiration.

The SP Lite2 is used for measuring solar radiation. It measures the solar energy received from the entire hemisphere i.e. 180° field of view. The output is expressed in Watts per square meter ( $W/m^2$ ). The SP Lite2 is designed for continuous outside use, and its calibration is valid only for unshaded natural daylight – not for artificial light. It is most usually used to measure solar radiation being received on the horizontal plane. However, the SP Lite2 can, if required, be used in an inverted or tilted position [35 ].

##### 3.9.1.1 Specifications of silicon pyranometer (SP lite 2)

Spectral range (overall)	400 to 1100 nm
Sensitivity	60 to 100 $\mu V/W/m^2$
Response time SP Lite2 (95%)	< 500 ns
Directional response (up to 80° with 1000 $W/m^2$ beam)	< 10 $W/m^2$
Temperature response SP Lite2	< -0.15 % / °C
Operational temperature range	-40 °C to +80 °C
Maximum solar irradiance	2000 $W/m^2$
Field of view	180 °

Table 3. 3 specification of silicon pyranometer

Good quality, reliable radiation data is extremely important for all activities in the solar energy sector. Photovoltaic (PV) and concentrating solar power (CSP) thermal systems may have slightly differing requirements, but they need accurate solar radiation information for the same reasons [17]. Efficient utilization of solar energy for systems designs and selection of components for agricultural, industrial, telecommunications and household applications require knowledge of the actual solar radiation reaching the

earth's surface at location of interest. Hence, in the process of collecting data pyranometer was used to measure the solar intensity reaching on earth's surface.

There is the scientific standard instrument used for measuring solar radiation. The World Meteorological Organization (WMO) and the International Standards Organization (ISO) define these types of instruments. In a solar monitoring station, solar radiation is measured in three ways:



Figure 3. 14 pyranometer with its multi meter

- **Global Solar Radiation:** is the sum of the beam and the diffuse solar radiation on a surface. The most common measurements of solar radiation are total radiation on a horizontal surface, often referred to as global radiation on the surface. A “Pyranometer” measures global Solar Radiation, which is a radiometer with a glass dome that has a hemispherical view of the whole sky.
- **Direct Solar radiation:** is the solar radiation received from the sun without having been scattered by the atmosphere. Beam radiation often referred to as direct solar radiation. The direct solar radiation is measured by a “Pyrheliometer.” This is a radiometer with a 5° view that is pointed accurately at the Centre of the sun by an automatic Sun Tracker. It only sees the sun and its aureole.
- **Diffuse Solar Radiation:** is scattered by aerosols in the atmosphere and reflected by clouds. It received from the sun after its direction has been changed by scattering by the atmosphere. Diffuse radiation is referred to in some meteorological literature as sky radiation or solar sky radiation. A Pyranometer mounted on a sun tracker with a shading mechanism to block the direct solar irradiance measures it.



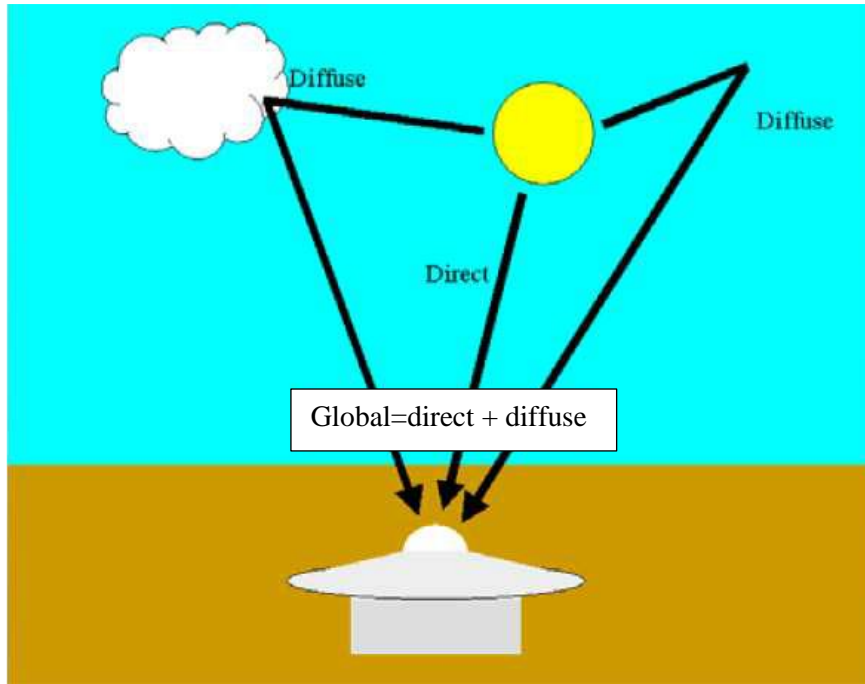


Figure 3. 15. World measurement organization solar radiation quantities

### 3.9.2 Infrared thermometer

It essentially consists of a lens to focus the infrared thermal radiation on to a detector, which converts the radiant power to an electrical signal that can be displayed in units of temperature after being compensated for ambient temperature. This permits temperature measurement from a distance without a contact with the object to be measured. A non-contact infrared thermometer is useful for measuring temperature under circumstances where thermocouples or other probe type sensors cannot be used or do not produce accurate data for a variety of reasons. It is also used to measure a high temperature where it is difficult to reach and make a contact.



Figure 3.16 infrared thermometer

### 3.10. Installation of the Scheffler Concentrator

While installing a Scheffler reflector at any site, the axis of rotation is fixed very precisely at an angle equal to “the latitude of the site” with horizontal in north-south direction. For daily tracking, these reflectors rotate along an axis parallel to polar axis with an angular velocity of one revolution per day to counterbalance the effect of daily earth rotation [1]. Scheffler reflectors are classified as standing reflectors and laying reflectors depending upon the direction of the concentrator face. All standing reflectors face towards south in the northern hemisphere, and north in the southern hemisphere, as well as providing focus at ground level. But the laying reflectors face north in the northern hemisphere, and south in southern hemisphere, as well as providing an elevated focus. The installation detail for standing reflectors in the northern hemisphere (at  $\theta^\circ$  latitude angle) is shown in Figure 3.17 below.

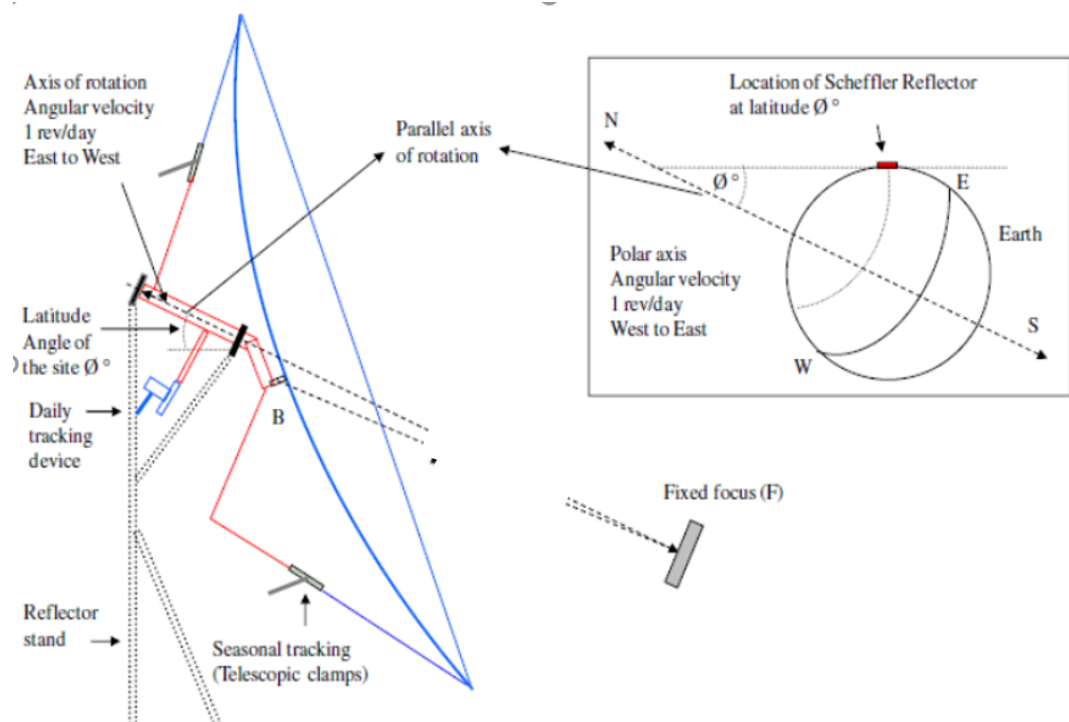


Figure 3.17 Installation and daily tracking details of Scheffler reflector (valid for standing reflectors in northern hemisphere)

### **3.11 Working principle**

The Scheffler reflector system works on the following principles:

- a. The Elliptic reflective dish turns about north-south axis parallel to earth's (South-North in Southern Hemisphere) axis, tracking by manual moment of disc, the sun's movement from morning (East) to evening (West), and maintaining gravitational equilibrium of the dish.
- b. The Elliptic reflector also performs change in inclination angle while staying directed to sun, in order to obtain sharp focal point.
- c. Focus lies at the axis of rotation. It remains at a fixed position, where the concentrated ray is captured and transferred to the coffee confined in the receiver.



## CHAPTER FOUR

### 4. ANALYSIS AND EXPERIMENTAL EVALUATION OF ELLIPTICAL DISH (SCHEFFLER) COFFEE ROASTER

#### 4.1 Solar irradiation

Solar irradiation is the amount of available solar energy on the ground surface over a specified time, expressed as kWh/m<sup>2</sup> or MJ/m<sup>2</sup>. Irradiance (1kWh/m<sup>2</sup> = 3.6 MJ/m<sup>2</sup>). The sum of direct and diffuse solar irradiation called global irradiation. Solar irradiation is important factor for the design and operation of the solar energy system [30].

		average day of month		
Month	n for ith day of the month	date	n	$\delta$
January	I	17	17	-20.9
February	31+i	16	47	-13
March	59+i	16	75	-2.4
April	90+i	15	105	9.4
May	120+i	15	135	18.8
June	151+i	11	162	23.1
July	181+i	17	198	21.2
August	212+i	16	228	13.5
September	243+i	15	258	2.2
October	273+i	15	288	-9.6
November	304+i	14	318	-18.9
December	334+i	10	344	-23

Table 4. 1 Recommended Average Days for Months and Values of n by Months [33]

#### 4.2. Available Solar radiation:

Since the measurements of solar radiation are often not available, attempts have been made by many investigators to establish relationship linking the values of the radiation (global or diffuse) with the metrological parameters like number of sunshine hours, cloud cover and precipitation.

##### 4.2.1 Monthly average daily global radiation:

To estimate monthly average daily global solar radiation on horizontal surface considers the following equation.

$$\frac{\bar{H}}{\bar{H}_0} = a + b\left(\frac{\bar{n}s}{\bar{N}s}\right) \quad (30)$$

$\bar{H}$  is the monthly average daily global solar radiation falling on a horizontal the surface at a particular location

$\bar{H}_0$  is the monthly mean daily radiation on a horizontal surface in the absence of the atmosphere

$\bar{n}s$  is the monthly mean daily number of hour of observed sunshine hours,

$\bar{N}s$  is the monthly mean value of day length at a particular location,

a, b - climatologically determined regression constant.

$$a = -0.110 + 0.235\cos\phi + 0.323 * \left(\frac{\bar{n}s}{\bar{N}s}\right)$$

$$b = 1.449 - 0.533\cos\phi - 0.694\left(\frac{\bar{n}s}{\bar{N}s}\right)$$

$\frac{\bar{n}s}{\bar{N}s}$  – is percentage of possible sunshine hour

**4.2.2. Monthly average daily diffuse radiation:** The monthly average daily diffuse radiation on a horizontal surface can be determined from the monthly average daily global radiation on a horizontal surface and the number of bright sunshine hours.

$$\frac{\bar{H}_d}{\bar{H}} = 0.931 - 0.814\left(\frac{\bar{n}s}{\bar{N}s}\right) \bar{H}_d = \bar{H} * [0.931 - 0.814\left(\frac{\bar{n}s}{\bar{N}s}\right)] \quad (31)$$

**4.2.3 Monthly Average Hourly Global Radiation on a Horizontal Surface:** The monthly average hourly global radiation on a horizontal surface can be calculated from the knowledge of the monthly average daily global radiation on a horizontal surface.

$$\frac{\bar{I}}{\bar{H}} = \frac{\pi}{24} (a + b\cos\bar{\omega}) * \frac{\cos\bar{\omega} - \cos\bar{\omega}_s}{\sin\bar{\omega}_s - \frac{\pi}{180}\bar{\omega} \cos\bar{\omega}_s} \quad (32)$$

Where

$$a = 0.409 + 0.5016\sin(\bar{\omega}_s - 60)$$

$$b = 0.6609 - 0.4767(\bar{\omega}_s - 60)$$

**4.2.4 Monthly Average Hourly Diffuse Radiation on a Horizontal Surface:** The monthly average hourly diffuse radiation on a horizontal surface can be calculated from the knowledge of the monthly average daily diffuse radiation on a horizontal surface.

$$\frac{\overline{Id}}{\overline{Hd}} = \frac{\pi}{24} * \left[ \frac{\cos \bar{\omega} - \cos \bar{\omega}S}{\sin \bar{\omega}S - \frac{\pi}{180} \bar{\omega}S \cos \bar{\omega}S} \right] \quad (33)$$

$$\overline{Id} = \overline{Hd} * \left( \frac{\pi}{24} \frac{\cos \bar{\omega} - \cos \bar{\omega}S}{\sin \bar{\omega} - \frac{\pi}{180} \bar{\omega}S \cos \bar{\omega}S} \right) \quad (34)$$

The ratio of average hourly total to daily total radiation as a function of hour relative to solar noon and the day length. The number of days is assumed symmetrical about solar noon and the hours indicated by their midpoints. In the present study, the monthly average hourly horizontal global and diffuse radiation for the given sunshine hours of Jimma city also calculated and plotted by the excel worksheet. The global solar radiation and diffuse solar radiation calculated from the following equation. Moreover, the direct normal radiation (beam) is the difference between global and diffuse radiation.

$$I * A_s * \alpha = h * A_s * (T_s - T_a) + \varepsilon * \sigma * A_s * (T_s - T_{sky}) \quad (35)$$

Where  $I$ ,  $\alpha$ ,  $\sigma$  and  $\varepsilon$  are solar radiation, absorptivity, Stefan Boltzmann constant and emissivity respectively.

The monthly average radiation outside of the atmosphere (extraterrestrial radiation on a horizontal surface)  $\overline{H_o}$  calculated as:

$$\overline{H_o} = 24 * \frac{360}{\pi} * I_{sc} \left( 1 + 0.033 \cos \left( \frac{360n}{365} \right) \right) \cos \phi \cos \delta \sin \omega S - \frac{\pi \omega S}{180} \sin \phi \sin \delta \quad (36)$$

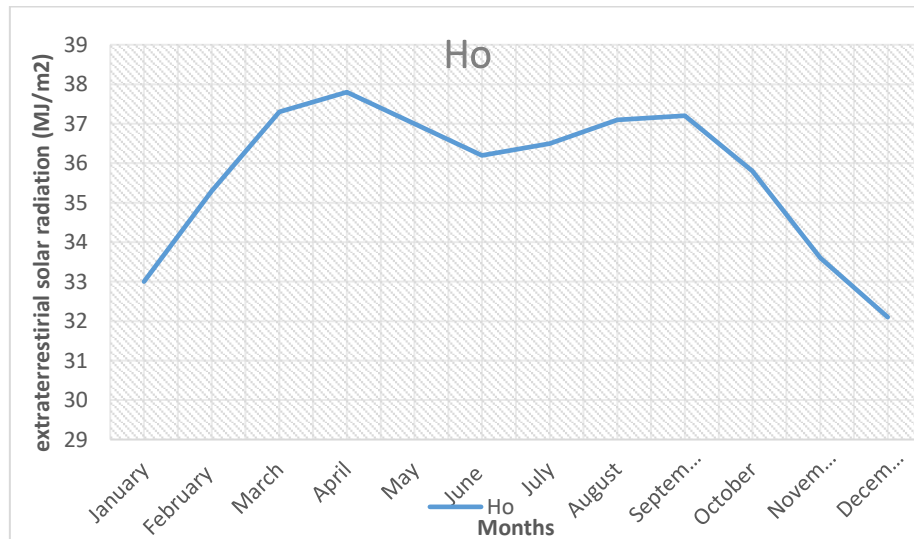


Figure 4. 1 monthly average Extraterrestrial radiation

The monthly mean value of day length at a particular location calculated as:

$$\overline{Ns} = \frac{2}{15^\circ} * \omega s \quad (37)$$

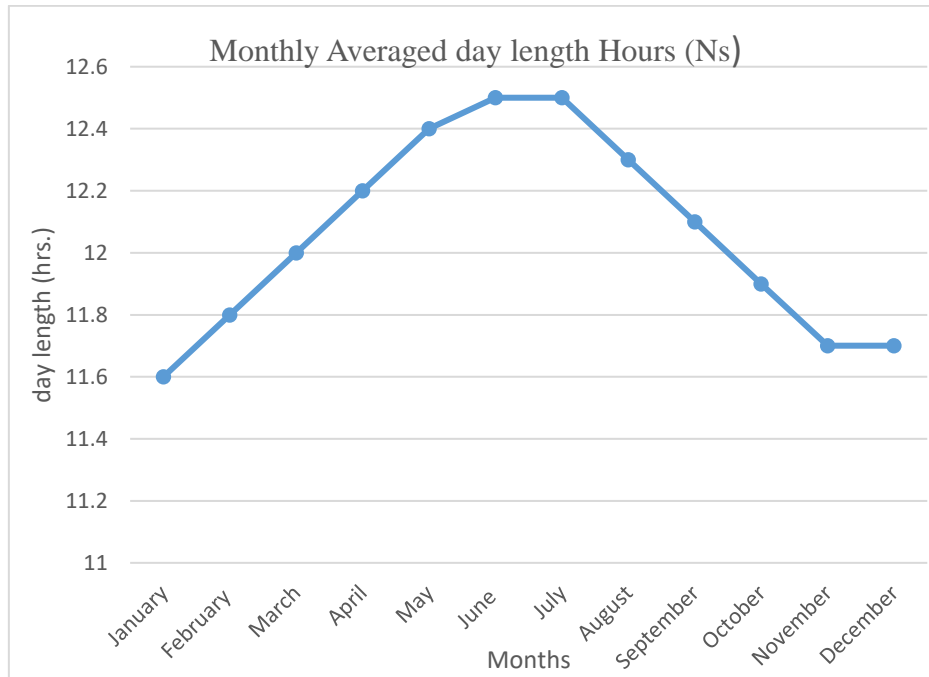


Figure 4. 2-Day length hours.

### 4.3 Solar angles

The time used in all of the sun-angle relations is the Solar Time. Solar time is a time based on the apparent angular motion of the sun across the sky, with solar noon the time with the sun crosses the meridian of the observer [4]. Watch time (Standard time) is described on longitudes and is dependent on the standard meridian for each country. The difference in minutes between solar time and standard time is given by

$$\text{solar time} = \text{standard time} + 4(Lst+Lloc)+E \quad (38)$$

Where:

Lst is the standard meridian for the local time zone

Local is the longitude of the location in question

E is equation of time E (in minutes)

$$E = 229.2(0.000075 + 0.001868 \cos B - 0.032077 \sin B - 0.014615 \cos 2B - 0.04089 \sin 2B)$$

$$B = (N - 1) \frac{360}{365} \quad (39)$$

**4.3.1 The hour angle ( $\omega$ ):** To describe the earth's rotation about its polar axis, we use the concept of the hour angle ( $\omega$ ). As shown in the figure below the hour angle is the

angular distance between the meridian of the observer and the meridian whose plane contains the sun. The hour angle is zero at solar noon (when the sun reaches its highest point in the sky). At this time the sun is said to be ‘due south’ (or due north in the Southern Hemisphere) since the meridian plane of the observer contains the sun. The hour angle increases by 15 degrees every hour [26].

The hour angle ( $\omega$ ). This angle is defined as the angle between the meridian parallel to sunrays and the meridian containing the observer [26]

*The Hour angle:* Hour angle is given by the following equation.

$$\omega = (ST - 12) * 15^\circ \text{ Where ST is solar time} \quad (40)$$

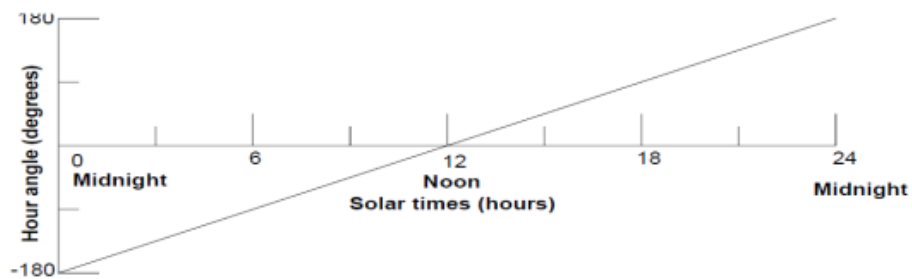


Figure 4. 3: hour angle Variation of the hour angle in a day [26]

**4.3.2 Declination angle ( $\delta$ ):** Declination angle is the angular position of the sun at solar noon (i.e., when the sun is on the local meridian) with respect to the plane of the equator, north positive and south negative,  $-23.45 \leq \delta \leq 23.45$ . the angle between the earth-sun line and the plane through the equator is called the solar declination angle ( $\delta$ ). The number of day  $n$  is from 1 to 365. Then the declination angle ( $\delta$ ) is calculated as follows.

$$\delta = 23.45 * \sin\left(360 * \frac{284+n}{365}\right) \quad (41)$$

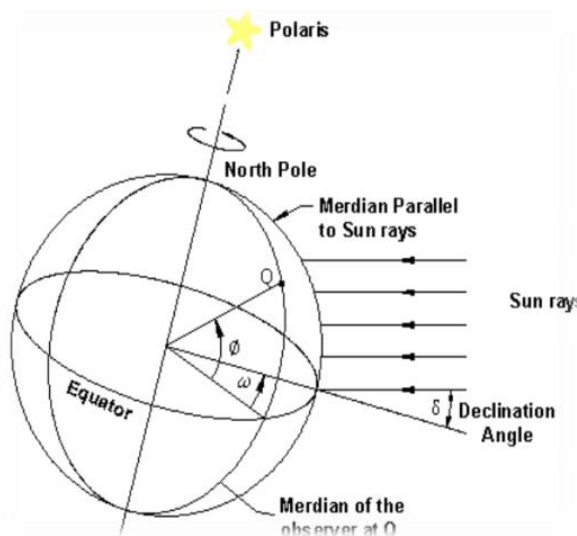


Figure 4. 4: declination angle of sunrays

The plane that includes the earth's equator is called the equatorial plane. If a line is drawn between the center of the earth and the sun, the angle between this line and the earth's equatorial plane is called the declination angle ( $\delta$ ). At the time of year when the northern part of the earth's rotational axis is inclined toward the sun; the earth's equatorial plane is inclined 23.45 degrees to the earth-sun line. At this time (about June 21), we observe that the noontime sun is at its highest point in the sky and the declination angle  $\delta = +23.45$  degrees. We call this condition the summer solstice, and it marks the beginning of summer in the Northern Hemisphere. As the earth continues its yearly orbit about the sun, a point is reached about 3 months later where a line from the earth to the sun lies on the equatorial plane. At this point, an observer on the equator would observe that the sun was directly overhead at noontime. This condition is called an equinox since anywhere on the earth, the time during which the sun is visible (daytime) is exactly 12 hours and the time when it is not visible (nighttime) is 12 hours. There are two such conditions during a year; the autumnal equinox on about September 23, marking the start of the fall; and the vernal equinox on about March 22, marking the beginning of spring. At the equinoxes, the declination angle ( $\delta$ ) is zero. The winter solstice occurs on about December 22 and marks the point where the equatorial plane is tilted relative to the earth-sun line such that the northern hemisphere is tilted away from the sun. We say that the noontime sun is at its "lowest point" in the sky, meaning that the declination angle is at its most negative value (i.e.,  $\delta = -23.45$  degrees). By convention, winter declination angles are negative. Declination ( $\delta$ ) can be found from the equation.

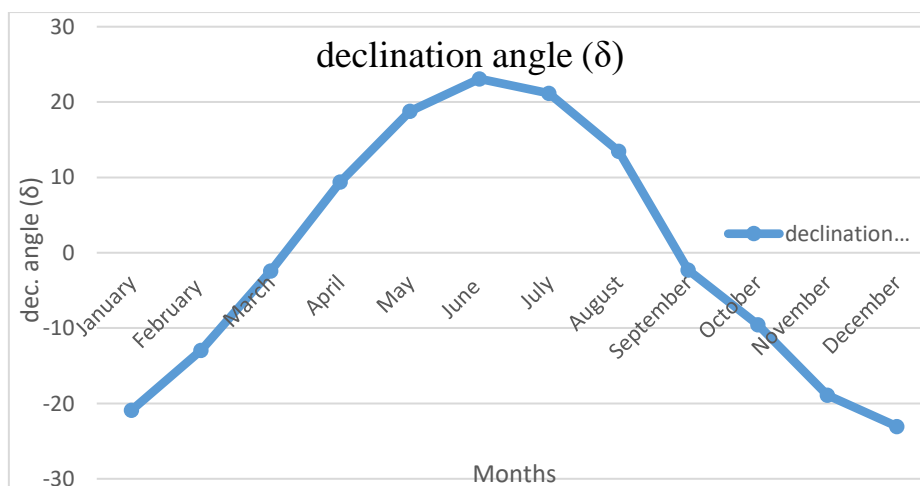


Figure 4. 5 variation of declination of angle for all months of the year where n is from table 4.

**Sunset hour angle is:**

$$\omega_s = \cos^{-1}(-\tan\phi \tan\delta) \quad (42)$$

$\phi$ =is altitude of Jimma, which is  $7.67^\circ$

$\delta$ =declination angle

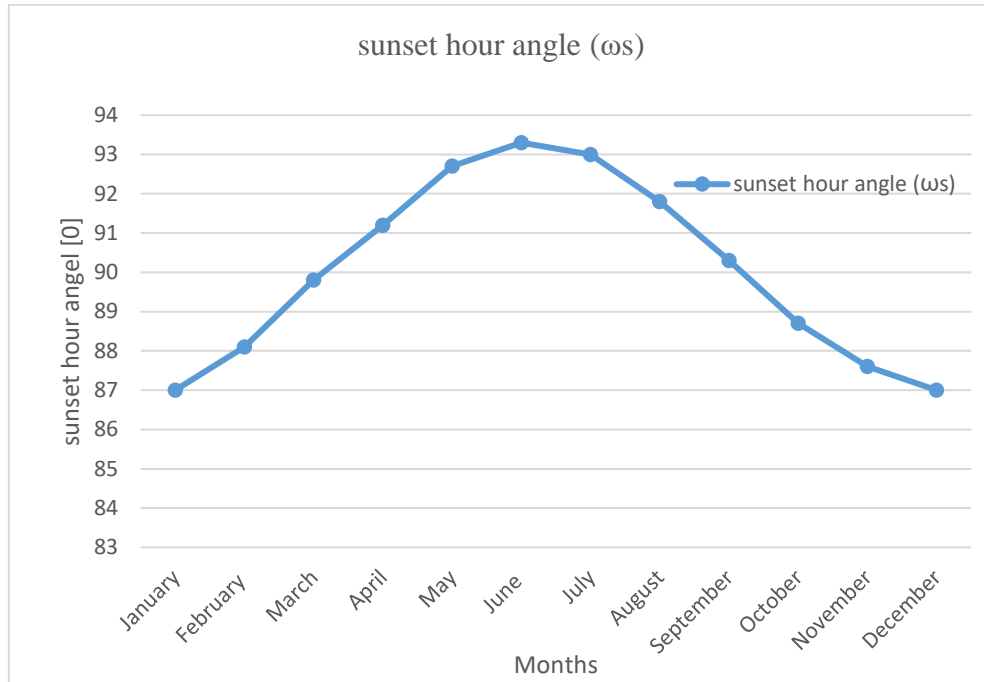


Figure 4. 6 sunset hour angle variation in months

#### 4.4 Data gathered during the experiment

The temperature data tabled below has measured from both absorber of scheffler reflector and parabolic dish. The parabolic dish of a diameter 1.8m that has a calculated focal length of 0.72m while the depth of the dish is 0.28m is used. The data from parabolic dish has taken only for the sake of comparing it with scheffler reflector's performance at the same time. The table shown below indicates the solar data i.e. temperature from receivers of both scheffler (elliptical dish) and solar dish collector. The time given is indicated based on Jimma local time. The other is the solar intensity at different height from the ground. The two data from the two table is taken at multiple days in February and March and the average data is received. The data in the following table has been collected on January 19/2020.

<b>local time (hr.)</b>	<b>Tr scheffler(°C)</b>	<b>Tr solar dish (°C)</b>	<b>Solar intensity (W/m<sup>2</sup>)</b>
11:10am	40	130	929.9
11:20am	55	149	960.4
11:30am	130	210	968
11:40am	160	140	983.2
11:50am	140	150	1006.1
12:00pm	180	180	1013.7
12:10pm	260	150	1021.3
12:20pm	225	155	1067.1
12:30pm	245	156	1082.3
12:30pm	270	160	1089.9
12:40pm	273	157	988
12:50pm	280	162	940
13:00pm	297	167	960.4
13:10pm	300	165	1067.1
13:20pm	276	150	1082.3
13:30pm	285	180	929
13:40pm	296	173	899.4
13:50pm	212	174	929.9
14:00pm	154	181	960.4
14:10pm	123	188	1006.1
14:20pm	67	195	1021.3
14:30pm	41	190	990.9

Table 5. 1 Data collected on January 19/2020

There are multi Solar data received during the assessment of scheffler coffee roaster, but for simplicity, two tables are selected since most of them have a similar to indication.



<b>time(hr.)</b>	<b>Tr scheffler (°C)</b>	<b>Tr dish (°C)</b>	<b>Solar intensity (W/m<sup>2</sup>)</b>
12:00pm	160	110	838.4
12:10pm	185	140	853.7
12:20pm	200	156	861.3
12:30pm	220	158	868.9
12:40pm	235	165	914.6
12:50pm	260	175	929.9
13:00pm	262	173	914.6
13:10pm	266	170	914.6
13:20pm	278	178	975.6
13:30pm	275	177	929.9
13:40pm	269	175	739.3
13:50pm	222	177	868.9
14:00pm	218	160	929.6
14:05pm	215	173	945.1
14:10pm	208	176	853.7
14:15pm	193	178	884
14:40pm	75	180	914.6

Table 5. 2 solar data collected on February 28/2020

#### **4.5 Why the ray from the elliptical dish was not focused**

After examining the dish, the following reasons are drafted why rays are not focusing appropriately.

- The North-South direction of the hourly and seasonal rotation of the dish was not considered appropriately (South-North direction in Southern Hemisphere)
- The two telescopic clamps are not fitting the exact hourly changes to compensate changes of sun's position during the day
- The receiver designed for coffee roasting does not transfer heat required all over its surface i.e. the reaction surface (the surface that the reflected ray strikes) is too small. It is multilayered and temperature lost is high.
- The engine that rotates the reflector following the sun's position is not positioned well.

Beyond the above four reasons, the reflector has no any other problem to function accordingly.

#### **4.6 Remedies taken**

Different measures have taken to harness the possible amount of energy from the reflector to roast coffee beans. These are:

- Finding the better ray focusing area by observing the reflector through assessment during the whole of sunny day. This measurement is done and the better result is gained as shown in the table.
- Changing the receiver that has a better reaction surface. The same material of receiver with previous is raised and the result is much better.
- Identifying the time at which the ray is focused and it is displayed using graphs.
- The parabolic solar dish collector was manufactured, and assessed with the scheffler reflector at the same time and the result is compared.

#### **4.7 Assessment procedure**

After a series of assessment procedure, positive results have been harnessed from the scheffler reflector. As seen in the above two tables the temperature recorded from the scheffler reflector is compared with temperature recorded from parabolic solar dish collector. However, the time of the day at which the maximum temperature harnessed from the elliptical dish (scheffler reflector) is minimum. As one can refer from the two the graphs above, the temperature of the receiver of coffee roaster rises from (11:00AM) in a short time and it declines at about (14:30 PM) local time. This shows the problem is not with the dish, but due to the error occurred during the installation time, the elliptical dish that has a fixed receiver in a design could not concentrate the beam radiation coming from the sun. During the morning (before 11:00AM) and afternoon (after 14:00PM) even if the day is sunny day there is no concentration of beam radiation i.e. the receiver cannot harness the temperature required for coffee roasting purpose. The time gap at which required amount of temperature gained is short. The time gap at which the required temperature is available is discovered during the assessment. The coffee is roasted at the available temperature to both scheffler dish and solar dish collector. The figures below was captured during the assessment.

Using the above results, the coffee grain has been roasted. As discussed above the defect happened during the installation of coffee roaster made the solar beam radiation not to concentrate. Not only this but also the design of receiver (the cylindrical shaped in which coffee is roasted) is not good enough to distribute the amount of heat required for roasting purpose. Hence, other type of cylindrical shaped receiver is raised. Figure 3 below is the newly selected receiver which 100% works for roasting coffee beans.



#### **4.8 Heat transfer analysis using Comsol Multiphysics**

Heat transfer analysis part has been done using comsol multiphysics software package. The amount of heat received by the receiver (roaster) at focus point is going to be analyzed in the following section. Heat transfer is involved in almost every kind of physical process, and can in fact be the limiting factor for many processes. Therefore, its study is of vital importance, and the need for powerful heat transfer analysis tools is virtually universal. Furthermore, heat transfer often appears together with, or because of, other physical phenomena. The modeling of heat transfer effects has become increasingly important in product design including areas such as electronics, automotive, and medical industries. Computer simulation has allowed engineers and researchers to optimize process efficiency and explore new designs, while at the same time reducing the need for costly experimental trials.

The Heat Transfer in Solids interface is used to model heat transfer in solids by conduction, convection, and radiation. A Solid model is active by default on all domains. All functionality for including other domain types, such as a fluid domain, is also available. The temperature equation defined in solid domains corresponds to the differential form of the Fourier's law that may contain additional contributions like heat sources. When this version of the physics interface is added, these default nodes are

added to the Model Builder Solid, Thermal Insulation (the default boundary condition), and Initial Values. Then, from the Physics toolbar, add other nodes that implement, for example, boundary conditions and sources.

### 4.8.1 Heat transfer in comsol multiphysics

**Conduction heat transfer:** - Conduction is a process of heat transfer generated by molecular vibration within an object. The object has no motion of the material during the heat transfer process. The example below well explained about conduction heat transfer.



Figure 4. 7 conduction heat transfer

As figure 4.7, there is a metal stick. Using a candle to heat the left side of the stick for a while, then the right side of the stick will be found to be hot as well. It is because the energy has been transferred from the left side of the stick to the right side. In addition, this kind of heat transfer is conduction. After knowing a subject's conduction is the heat transfer from one end to the other end, it is important for calculating about the heat transfer rate. Based on the experiment experiences, for the one dimension conduction heat transfer in a plane wall, the amount of heat energy being transferred per unit time is proportional to the normal temperature gradient  $\frac{dT}{dx}$  and the cross-sectional area A [7]

$$q = -kA \frac{dT}{dx} \quad (43)$$

Where q is the heat-transfer rate (W), A is cross-sectional area (m<sup>2</sup>), k is the thermal conductivity of the material (W/ (m.K)),  $\frac{dT}{dx}$  is the temperature gradient. The Equation (1) is the formula of calculation of conduction heat transfer rate; it is also known as Fourier's law of heat conduction. The minus sign means heat transferred in the direction of decreasing temperature. If the heat transfer rate q divided by the cross sectional area A, the equation (1) can be derived as:

$$q'' = -k \frac{dT}{dx} \quad (44)$$

Where  $q''$  is called conduction heat flux. The heat flux was derived from the Fourier's law of heat conduction; it can be described as the heat transfer rate through unit cross sectional area. The amount of the thermal conductivity  $k$  indicates the substance's ability of transferring heat. If it is a big amount, it means the substance has high level of ability on heat transfer. The number of the thermal conductivity depends on the material; of course, it is also affected by the temperature outside.

The Heat Transfer in Solids Interface solves for the following equation

$$\rho C_p \left( \frac{\partial T}{\partial t} + U_{trans} * \nabla T \right) + \nabla * (q + q_r) = -\alpha * T \frac{ds}{dt} + Q \quad (45)$$

The different quantities involved here are recalled below:

- $\rho$  is the density (SI unit: kg/m<sup>3</sup>)
- $C_p$  is the specific heat capacity at constant stress (SI unit: J/(kg·K))
- $T$  is the absolute temperature (SI unit: K)
- $U_{trans}$  is the velocity vector of translational motion (SI unit: m/s)
- $q$  is the heat flux by conduction (SI unit: W/m<sup>2</sup>)
- $q_r$  is the heat flux by radiation (SI unit: W/m<sup>2</sup>)
- $\alpha$  is the coefficient of thermal expansion (SI unit: 1/K)
- $S$  is the second Piola-Kirchhoff stress tensor (SI unit: Pa)
- $Q$  contains additional heat sources (SI unit: W/m<sup>3</sup>)

For a steady-state problem, the temperature does not change with time and the terms with time derivatives disappear. However, in this thesis since the analysis of heat transfer in receiver of the (roaster) is time dependent. Therefore, the above equation will be as it is, No term of the equation will be disappeared. The first term on the right-hand side of Equation 4 is the thermos-elastic damping and accounts for thermo-elastic effects in solids:

$$Q_{ted} = -\alpha * T \frac{dS}{dt} \quad (46)$$

It should be noted that the  $d/dt$  operator is the material derivative, as described in the Time Derivative subsection of Material and Spatial Frames.

# CHAPTER FIVE

## 5. SIMULATION AND RESULT

### 5.1 simulation of data gathered

Solar data collected during the assessment, which is labeled in the above section can be more clarified by showing it in the graphs. After a series of assessment procedure, positive results have been harnessed from the scheffler reflector. As shown in table 5.1 and 5.2, the temperature recorded from the scheffler reflector is compared with temperature recorded from parabolic solar dish collector. However, the time of the day at which the maximum temperature harnessed from the elliptical dish (scheffler reflector) is minimum. As one can refer from the two the graphs above, the temperature of the receiver of coffee roaster rises from (5:00AM) in a short time and it declines at about (8:30 PM) local time.

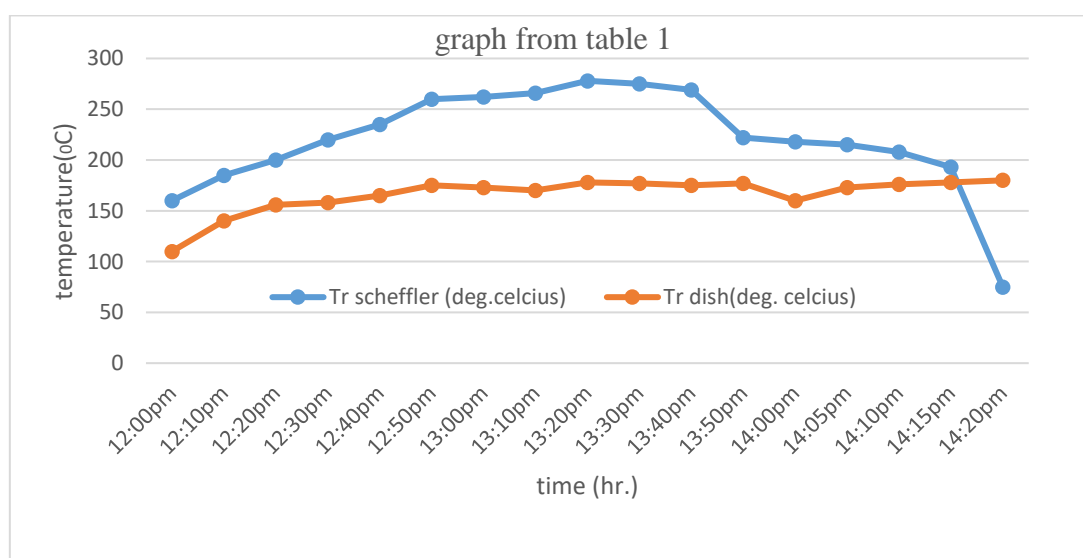


Figure 5. 1 comparison data from both scheffler and parabolic dish

This shows the problem is not with the dish but due to the North South positioning error occurred during the installation time, the elliptical dish that has a fixed receiver in a design could not concentrate the beam radiation coming from the sun. During the morning (before 5:00AM) and afternoon (after 14:00PM) even if the day is sunny day there is no concentration of beam radiation i.e. the receiver cannot harness the temperature required for coffee roasting purpose. The time gap at which required amount of temperature gained is short. The time gap at which the required temperature

is available is discovered during the assessment. The coffee is roasted at the available temperature to both scheffler dish and solar dish collector.

Since the installation defect happened, the dish could not concentrate the beam radiation. However, after series of attempts to make the concentration happened, results have been gained. As shown below, the temperature needed to roast coffee has been harnessed. As the result is simulated using the comsol multiphysics software package. Calculating the heat flux and putting the result in comsol multiphysics, processing the simulation the temperature distribution on the receiver has been gained in figure 5.4. The temperature versus time is also a result we can extract from the Comsol Multiphysics software package as indicated in figure 5.5.

In a similar way, the graph from the table 5.2 is plotted below as the shape of it is nearly similar with the figure 5.1 and the temperature of the scheffler receiver rises during mid-day and falls during the afternoon from the two graphs.

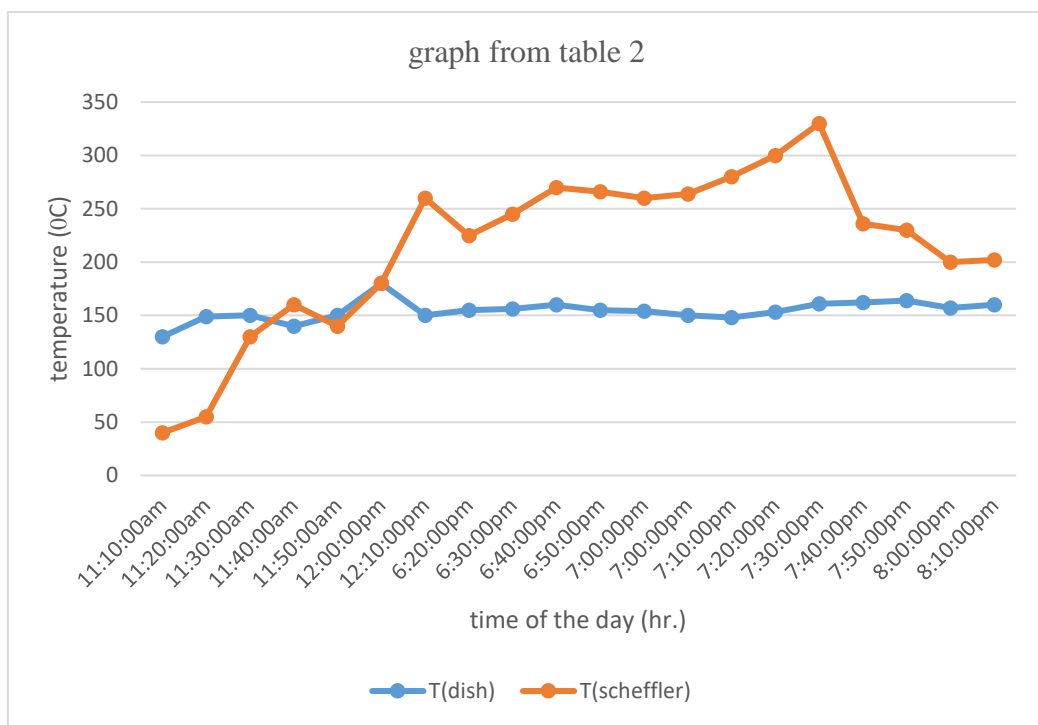


Figure 5. 2 comparison data from both scheffler and parabolic dish

## 5.2 Simulation using comsol multiphysics

### 5.2.1 Meshing Concepts

After constructing 3D of the receiver in comsol multiphysics, the process of applying boundary conditions to the simulation process is important. The Mesh nodes enable the discretization of the geometry into small units of simple shapes, referred to as mesh elements. A mesh is the result of building a meshing sequence. A meshing sequence corresponding to a geometry consists of Meshing Operations and Attributes. The attribute nodes store properties that are used by the operation nodes when creating the mesh. Building an operation node creates or modifies the mesh on the part of the geometry defined by the operation node's selection. Some of the operation nodes use properties defined by attribute nodes; for example, the Free Tetrahedral node reads properties from the Distribution and Size attribute nodes [26]. If you choose to import a mesh, you have access to a different set of operations. For some operation nodes, you can right-click to add local attribute nodes as sub nodes. Properties defined in local attribute nodes of an operation node override the corresponding properties defined in global attribute nodes (on the same selection.)

In 3D geometries, the mesh generator discretizes the domains into tetrahedral, hexahedral, prism, or pyramid mesh elements whose faces, edges, and corners are called mesh faces, mesh edges, and mesh vertices, respectively. The boundaries in the geometry are discretized into triangular or quadrilateral boundary elements. The geometry edges are discretized into edge elements. Similar to 2D, the geometry vertices are represented by vertex element.

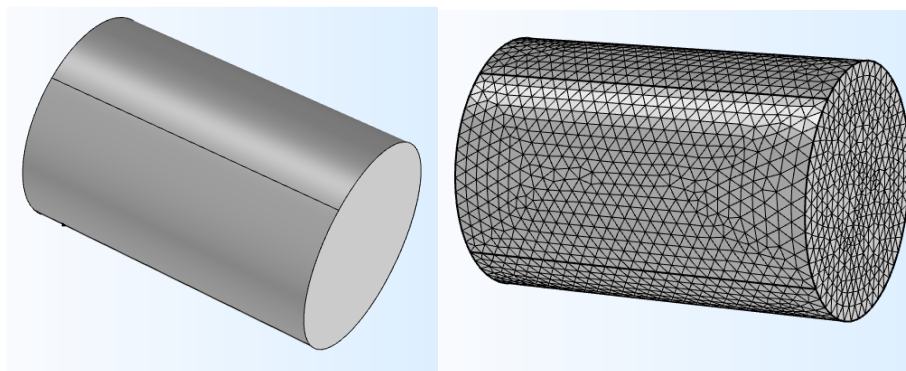


Figure 5. 3 mesh of scheffler receiver

Parameter of the receiver (cylinder) like height, which is 0.45m, diameter of the cylinder 0.3m and from the boundary conditions ambient temperature of Jimma that is



28<sup>0</sup>C is provided to the comsol multiphysics software. In addition, another important parameter called heat flux ( $q''$ ) calculated below has been provided to the software.

$$\text{General inward heat flux} = \text{concentration ratio} * \text{solar flux}$$

Where average solar flux is 992W/m<sup>2</sup> and concentration ratio is 8.

$$q'' = 8 * 992 \text{ W/m}^2$$

$$q'' = 7936 \text{ W/m}^2$$

The below figure shows the temperature distribution on the receiver. As one can refer from the figure, maximum temperature of 152<sup>0</sup>C can be gained which is above the required amount during in 500 seconds of operation.

According to the analysis in comsol multiphysics, there is no thermal insulation on the roaster (receiver) surface and ambient temperature of 28<sup>0</sup>C is given as an initial values, therefore convective heat loss exists on roaster surface.

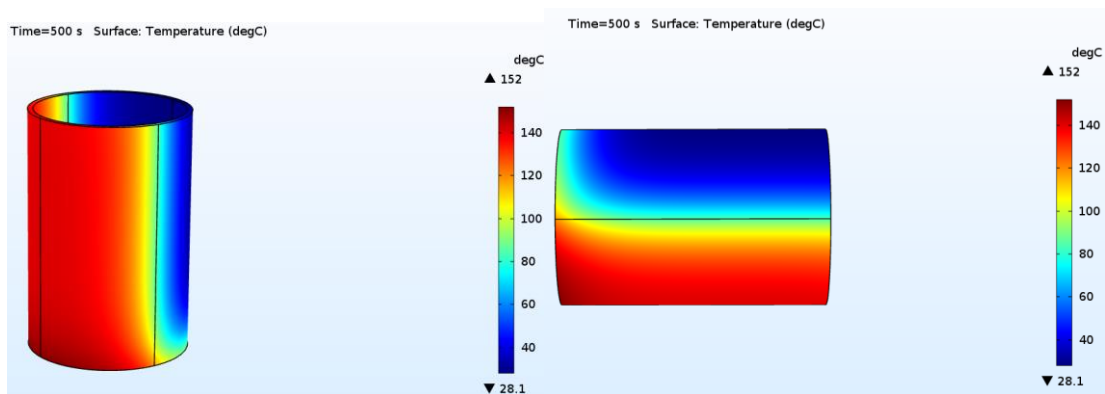


Figure 5. 4 temperature distribution on receiver surface

The figure 5.5 below also shows the temperature and time relation. In time dependent analysis, the progress of temperature distribution during each 0.1 second looks the following figure.

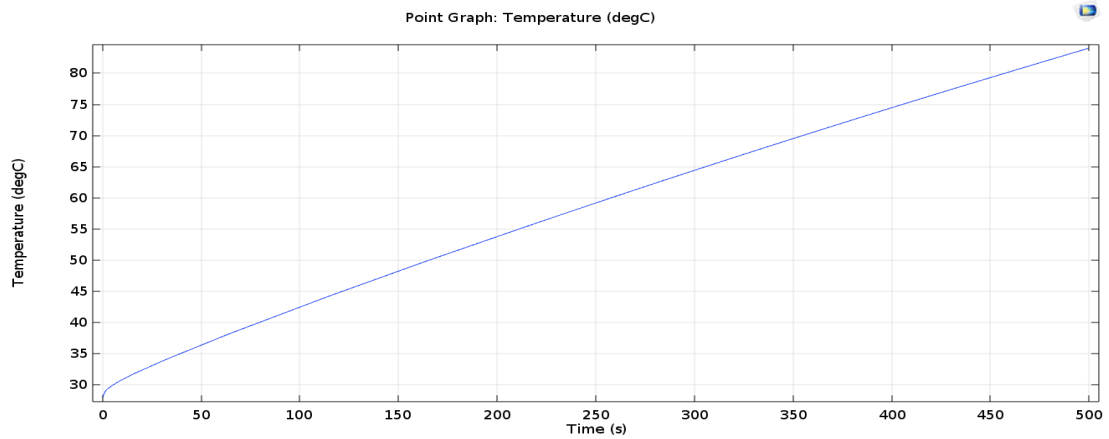


Figure 5. 5 temperature distribution with time

As shown in the figure below, the coffee has been roasted after the required amount of temperature is incurred on the absorber. The bigger absorber is not proper enough to absorb and deliver the heat required to a coffee bean due to its small absorbing area and its design complexity. The following pictures were captured during the roasting is in progress.

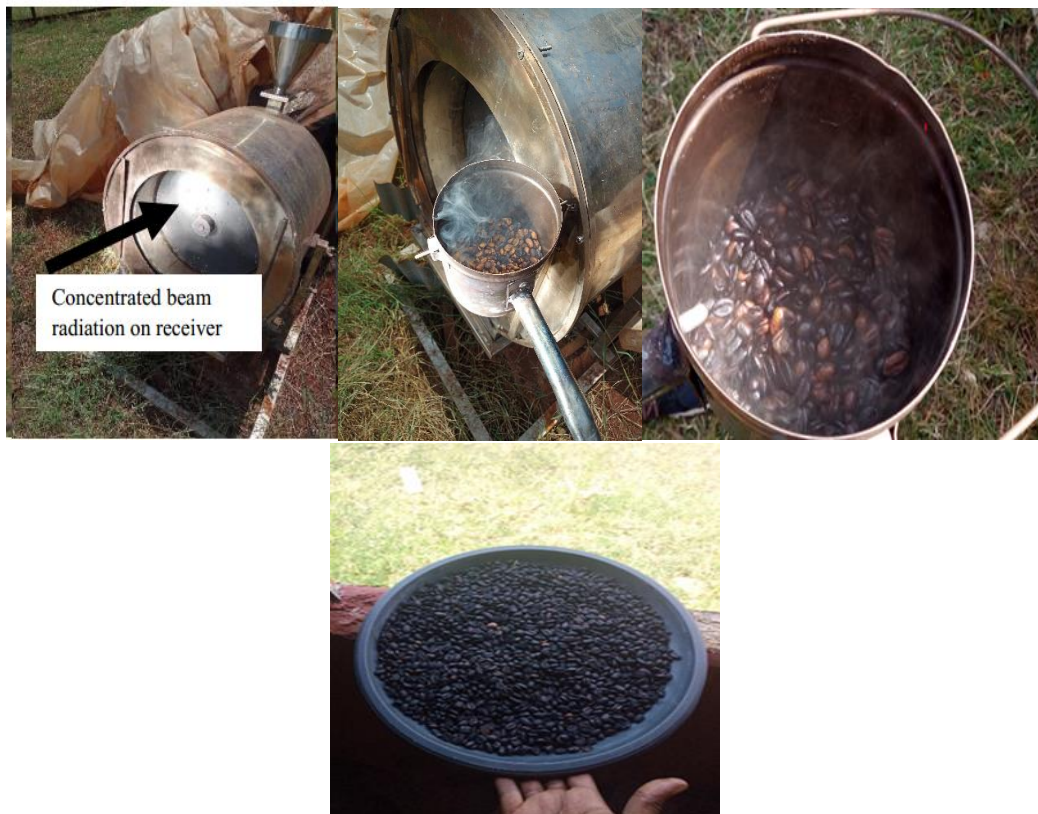


Figure 5. 6 Roasting coffee using scheffler reflector

### 5.3 Interpretation of the result

When the two graphs are observed, even if the data they represent is taken at the different days, the outcome is nearly similar. The two graphs show comparison of parabolic solar dish and elliptical dish concentrators. The temperature level on the graph is taken from the receivers of both dishes. The curve on both graphs of scheffler reflector and parabolic solar dish are expressed below.

***Parabolic solar dish:*** - The temperature which will be gained at the focus point has no big difference irrespective of time and solar angle, because tracking mechanism of the parabolic solar dish is performed manually until maximum possible amount of temperature is gained at the focus point (see the two graphs above). Since its tracking mechanism is done manually solar angle and position of the sun does not affect the temperature gained at focus point. This is good for a long time operation during the sunny day. The maximum temperature of 200<sup>0</sup>C have found from the parabolic solar dish. The advantage of parabolic solar dish is that uniform temperature and maximum operational time since its tracking mechanism is manually.

***Scheffler (elliptical dish):*** - the curve, which indicates the temperature recorded throughout the day from the receiver of scheffler reflector is small during the morning time and becomes large during the mid-day. Because the reflected solar beam will be concentrated during the mid-day and it disperses after 14:30 PM. Since the focus of the scheffler reflector is fixed, type in design, there is no option for manual tracking as parabolic solar dish. The reason for this is that the reflector has not installed appropriately according to the manufacturer's manual. The rotation of the dish for daily tracking and telescopic clamps are not exactly working as referred from the manual. So, the working time for scheffler reflector coffee roaster is finally fixed from 11:00AM-14:30 PM local time. On a sunny day, maximum temperature of up to 330<sup>0</sup>C were recorded which is good enough for roasting coffee. The advantage of scheffler reflector is that maximum temperature have harnessed from it where the operation time is too short.

## CHAPTER SIX

### 6. CONCLUSION AND RECOMMENDATION

This chapter is the last part of the thesis and focuses on the summary to formulate the conclusion and recommendation for the future work to enhance the research.

#### 6.1 conclusion

The work presented here in this thesis has been to adjust and enhance the elliptical dish (scheffler reflector). The following conclusions are drawn from the research work:

- After assessments, the incorrectly installed scheffler reflector has been partially adjusted. Hence, temperature of 152<sup>0</sup>C is achieved which is good enough to roast coffee.
- The performance of scheffler reflector is much better than parabolic solar dish. If scheffler reflector is properly installed, its performance will be huge than parabolic solar concentrator according to the data simulated for the two solar concentrators.
- In simulating the result, the nature of boundary condition plays an important role on amount of heat lost.
- Providing surface heat flux, ambient temperature and the size of the mesh has also a significant impact on results.
- The analysis which done by default setting will lead us to a wrong result, therefore every parameters has be given to the Comsol multiphysics based on the data gathered from the site.

## 6.2 Recommendation

Many corrective measures have taken to make the scheffler reflector concentrate the solar beam coming from the sun. Certain activities that has to be considered when manufacturing and installing scheffler reflector are recommended below:

- Using properly working telescopic clamps
- Using improved facets of glass mirror
- Replacing the receiver that has a better heat transfer and better surface reaction to apply heat flux.
- North-south direction is another important point because the dish has to be rotated along the north-south direction, to compensate the hourly changing of sun's position. During the day, the dish has to be rotated  $15^{\circ}$  in every hour to get a better solar beam.

Generally, a single layered receiver has to be used for a better temperature distribution than a multilayered one. Roasting coffee using such a technique does not seem better due to the temperature fluctuation based on whether the sky is clear or not.

When the temperature is high in a receiver (up to  $152^{\circ}\text{C}$ ), the heat distribution in the surface of the coffee bean is not similar. Its outer part will burned while there is no color change at the core. This is not good to make a good taste coffee. Hence, it will be good to use scheffler reflector for other purposes like heating, boiling and small-scale power generations. Therefore, there are other options that we can for see since the scheffler reflector was not designed for specific purposes. Anyone who wants make this project better can simply work designing the receiver according to the required application.

## References

- [1] Munir, O. Hensel, W. Scheffler, “Design Principal and Calculations of Scheffler fixed focus Concentrator for Medium Temperature Applications.
- [2] Jose Ruelas, Nicolas Velazquez, Jesus Cerezo, “A Mathematical Model to develop a Scheffler-Type Solar Concentrator Coupled with Sterling Engine”
- [3] Rupesh J. Patil, G. K. Awari, Mahendra Prasad Singh, “Performance Analysis of Scheffler Reflector and Formulation of Mathematical Model”, VSRD-TNTJ, Vol.2 (8), 2011, 390-400
- [4] Vishal R. Dafle, Prof N. N. Shinde, “ Design, Development and Performance Evaluation of Concentrating Monoaxial Scheffler Tehnology For Water heating and Low temperature Industrial Steam Application”,IJERA, vol.2, Issue 6, 2012, pp. 848-852
- [5] Regin AF, Solanki SC, Saini JS. Heat transfer characteristics of thermal energy storage system using PCM capsules: a review. *Renew Sustain Energy Rev* 2008;12 (9):2438–58
- [6] Solar Energy Solar PV (for electricity) and Thermal (for hot water) Systems, (<http://www.yesweb.org/docs/solarenergy.pdf>) (Accessed on 12th December, 2015).
- [7] Ummadisingu, Amita, S. Concentrating solar power- Technology, potential and policy in India.
- [8] International journal of advnaced technology and innovative research, IISN- 2348-2370, Vol. 7, August 2015, (<http://www.ijatir.org/uploads/163452IJATIR6353-305.pdf>).
- [9] Solar (PV and CSP). (<http://www.iea.org/topics/solarpvandcsp>). Accessed on (18<sup>th</sup> December, 2015)
- [10] Dimroth F, Grave M, Beutel P, Fiedeler U, Karcher C, Tibbits TN, Oliva E, Siefer G, Schachtner M, Wekkeli A, Bett AW. Wafer bonded four-junction GaInP/GaAs//GaInAsP/GaInAs concentrator solar cells with 44.7% efficiency. *Progr Photovolt: Res Appl* 2014; 22 (3):277–82
- [11] Gregor Schapers, “Agave syrup production – a sweet tradition goes solar”, International Solar Food Processing Conference 2009

- [12] Christoph Müller, “Solar community bakeries on the Argentinean Altiplano”, International Solar Food Processing Conference 2009
- [13] Munir A, Hensel O. Biomass energy utilization in solar distillation system for essential oils extraction from herbs. In Conference of international research on food security, natural resource management and rural development, University of Hamburg; 2009 Oct
- [14] Jayasimha BK, Akashwani O, Hadapsar P. Application of Scheffler reflectors for process industry. In: Proceedings of international conference on solar cooker, Spain 2006 July (p. 15–6)
- [15] Melkamu Yayejew; *Integration of scheffler concentrator and thermal storage device for indoor Injera baking*, Addis Ababa University April 2013.
- [16] John A. Duffie; William A. Beckman *Solar Engineering of Thermal Processes*, Fourth Edition, 2013.
- [17] Kipp and Zonen; *solar radiation measurements for solar energy applications*, since 1830 Davos Switzerland.
- [18] Leland and Mansoori, *Basic Principles of Classical and Statistical Thermodynamics*, University of Chicago, p. 1
- [19] Songer and Associates Inc. *A Thermodynamic Approach to Roasting Parameters and Stages of Roast*, 2012.
- [20] Eggers and Pietsch, “Technology I: Roasting”, *Coffee: Recent Developments*, 2001, Blackwell Science Limited, London, p. 90.
- [21] Schenker, et al. “Impact of Roasting Conditions on the Formation of Aroma Compounds in Coffee Beans,” *Journal of Food Science*, Vol. 67, No. 1, 2002, Institute of Food Technologists, p.
- [22] Eggers, R. “Heat and Mass Transfer during Roasting –New Process Developments,” 19<sup>th</sup> International Scientific Colloquium on Coffee, 2001, Association Scientifique du Café, Paris, p.7
- [23] Hobbie and Eggers, “*The Influence of Endothermic and Exothermic Energies on the Temperature Field of Coffee Beans during the Roasting Process*,” 19<sup>th</sup>

International Scientific Colloquium on Coffee, 2001, Association Scientifique du Café, Paris,

[24] Anil Kumar, “*A comprehensive review of Scheffler solar collector*” Prince of Songkla University 2017, Hat Yai, Thailand.

[25] Desireddy Shashidhar Reddy “*Design and ray tracing of multifaceted Scheffler reflector with novel crossbars*” 2019, Indian Institute of Technology Patna, India.

[26] COMSOL Multiphysics Reference Manual version 5.3 2019

[27] Tarekegne, Melaku, “*Designing and Experimental Investigation of Scheffler reflector based solar distiller for Sesame Seed Oil Extraction*” Bahir dar institute of technology school of research and postgraduate studies November 14, 2018 Bahir dar, Ethiopia.

[28] S. Kumar, V. Yadav, U. Sahoo\*, S.K. Singh “*Experimental investigation of 16 square meter Scheffer concentrator system and its performance assessments for various regions of India*” National Institute of Solar Energy, Gurgaon, Haryana 122003, India 2019.

[29] Rupesh, J. et al., 2011. “Prasad Singh Performance Analysis of Scheffler Reflector and Formulation of Mathematical Model”; <http://www.solare-bruecke.org>

[30] Scheffler, W., 2006. “Introduction to the revolutionary design of Scheffler”; In: SCIs International Solar Cooker Conference, Granada, Spain

[31] [www.wlv.com/products/databook,2011](http://www.wlv.com/products/databook,2011). “Wolverine tube Heat Transfer”; Tata Book

[32] Medwell mg Journals, 2009; “Comparison of Thermal Energy Storage Techniques”; <http://www.medwelljournals.com>

[33] John A. Duffie and William A. Beckman “*Solar Engineering of Thermal Processes*” 2013

[34] SP lite silicon pyranometer instruction manual revision 2004

[35] Scheffler, W., 2006. “Introduction to the revolutionary design of Scheffler”; In: SCIs International Solar Cooker Conference, Granada, Spain



## Appendix



(a)

(b)

Fig. (a)Scheffler dish installed at JUCAVM (b) receiver (absorber)



Fig. Temperature on absorber



Fig. Coffee roasted during the experiment



Fig. Pyranometer and its digital multi meter





Fig. infrared thermometer